STATE ESTIMATION IN ACTIVE DISTRIBUTION SYSTEMS:

Comparison Between Weighted Least Squares and Extended Kalman Filter Algorithms

Prepared by:
Jeff Kimasere Watitwa

Supervised by:
Mrs Kehinde Awodele
Department of Electrical Engineering
University of Cape Town

Dissertation submitted in partial fulfillment of the requirements for the degree of Master of Science in Electrical Engineering

July 2021

Declaration

1. I know that plagiarism is wrong. Plagiarism is to use another's work and pretend that it is one's own.

2. I have used the IEEE convention for citation and referencing. Each contribution to, and quotation in, this dissertation from the work(s) of other people has been cited and referenced.

3. This report is my own work.

4. The dissertation does not exceed the specified limit of 30,000 words.

Signature:.....
J.K. Watitwa

Date: **December 29, 2021**

Acknowledgments

To God be the glory.

Firstly, I would like to express my sincere gratitude to my supervisor Mrs Kehinde Awodele for the continuous support of my Masters study, for her patience, motivation, and immense knowledge. Her guidance helped me during my research and dissertation write-up. I could not have imagined having a better advisor and mentor.

Besides my supervisor, I would like to thank the rest of the Power Systems Research Group: Prof. CT Gaunt, Prof. Komla Folly, and Dr. David Oyedokun, for their insightful comments and encouragement, but also for their hard questions which helped me to improve my research.

I thank my fellow colleagues for the stimulating discussions, shared resources and knowledge, and for all the fun and memories we have had in the last two years. Also, I thank my friends: Desire, Ntsiki, Eke, Keletso, Kingsley and Bright. In particular, I am grateful to the MasterCard Foundation Scholarship at the University of Cape Town for providing me a family away from home and the much needed financial support throughout my Masters studies.

Last but not the least, I would like to thank my family: Aunty Emily, Rachael, Hilda, Lucy and Mike for supporting me emotionally throughout the writing this dissertation and my my life in general.

Dedication

An apple does not fall far from its tree. I am my father's son.

I dedicate this dissertation to my father,the late Mwalimu Ben Wanjala Watitwa, and my mother, the late Madam Gladys Naliaka Watiwa; who generously gave me the gift of education and life.

Abstract

Distributed Generation units (DGs) have been continuously deployed since the early 1990s in distribution power systems to mitigate greenhouse gas emissions and climate change. Therefore, distribution systems, which were designed initially as passive networks, with little monitoring, are evolving into active networks, forcing Distribution System Operators to implement newer control applications in Distribution Management Systems (DMS). Distribution System State Estimation (DSSE) is a crucial component in DMS. DSSE is the process of obtaining the nodal voltage magnitude and its respective phasor angle in real-time by utilizing available recorded measurements and the parameters from the network topology. The state estimator's outputs are then used to realize appropriate monitoring and control for the distribution networks. Potential applications include optimal voltage and VAR control, DERs dispatch, islanding operation, and fault detection and location.

Transmission System State Estimation (TSSE) has been developed and applied since the late 1960s. However, TSSE methods are not directly transferable to distribution networks (DNs) since they differ in their design, topology and operation. DNs have distinctively shorter lines with higher Resistance to Reactance ratio, and single-phase and unbalanced three-phase circuits and loads. Importantly, scarcity of measurements in DNs present tremendous challenges in DSSE. Despite these challenges, pioneering work in DSSE commenced in the 1990s. The motivation of this research is to extend this work by comparing the performance of the Weighted Least Square (WLS) and the Extended Kalman Filter (EKF) state estimation algorithms in active DNs.

This dissertation develops and tests the performance of active distribution system state estimation WLS and EKF algorithms that consider the integration of DGs in standard IEEE-bus test feeders. An important contribution of this dissertation consists in the validation of the theoretical state estimation findings via the use of real-life data. The ADRES-CONCEPT project data were used to simulate real-time measurements, while the Particle Swarm Optimization algorithm was used to place the DGs and PMUs on the best possible nodes of the selected test system.

This dissertation starts by reviewing the state-of-the-art in DSSE, and provides the measurement and process model of the WLS and the EKF algorithms. Then, it illustrates the analytical formulation of the two algorithms as a function of the input measurements. Finally, a case studies on modified IEEE-33 bus and IEEE-69 bus test feeders were carried out on

MATLAB/OpenDSS software, and numerical evaluation and results are presented. The EKF algorithm out-performs the WLS algorithm with an average RMS error of 0.00020588 to 0.00025168. Similarly, EKF converges in 3 iterations, while WLS converges in 4.

Preceding this dissertation some of the research findings were published and presented in the 2019 and 2020 Southern Africa Universities Power Engineering Conferences and the 2020 Power Africa Conference.

Keywords

Active distribution networks, Weighted least squares, Extended kalman filter, Phasor measurement units, Active distribution system state estimation, DG placement, Particle swarm optimization algorithm.

Contents

List of Figures

List of Tables

List of abbreviations

PSSE	Power System State Estimation
ADMSs	Advanced Distribution Management Systems
DSSE	Distribution System State Estimation
ADSSE	Active Distribution System State Estimation
DNs	Distribution Networks
ADNs	Active Distribution Networks
DG	Distributed Generator
WLS	Weighted Least Square
EKF	Extended Kalman Filter
PMU	Phasor Measurement Unit
PSO	Particle Swarm Optimization
AMI	Advanced Metering Infrastructure
RTU	Remote Terminal Unit
PDC	Phasor Data Concentrator
BCSE	Branch Current State Estimation
NVSE	Nodal Voltage State Estimation
IED	Intelligent Electronic Devices
DER	Distributed Energy Resources
DSO	Distribution Systems Operators

Chapter 1

Introduction

1.1 Background to the study

Power System State Estimation (PSSE) is the mathematical process that determines the system's nodal voltage magnitudes and phase angles from redundant measurements and the existing network topology [1]. PSSE is important for power system monitoring, operation, and control. In the state estimation problem, only the slack/reference bus voltage is assumed to be known (1 p.u), and its phase angle is set at zero degrees, while the measurement devices are assumed to have an error. The inputs to the state estimator are composed of:

- Distributed measurements (power injections, load flows, line current, voltages)
- Pseudo-measurements or Load forecasts
- Existing Network topology and model

The state estimator calculates the most feasible solution of the nodal voltage magnitudes and phase angles of the power network from these inputs.

If the available real-time measurements are sufficient to allow an accurate prediction of the state variables, the system is said to be observable. Otherwise, it is unobservable [2]. For observability, it is necessary to have twice as many measurements as the number of nodes. State estimation is impossible in an unobservable system, and additional information such

as load forecast from historical data or additional measurement points is necessary to make the system observable. An observable system allows the state estimator to be resilient to erroneous measurements as it will be easy to filter out outlier measurements. Bad data detection and network correction are not possible without redundancy in the measurement of the system. In essence, the state estimator determines the most likely state by minimising the discrepancy between the redundant measurements and the underlying network topology [3].

While state estimation is the better option to ensure complete system visibility, it is not the only method. Many utilities still use load flow analysis to predict the internal system state based on power injections and customer load forecasts during network planning and design. The introduction of real-time measuring infrastructure like PMUs in distribution networks has contributed to the establishment of advanced distribution management systems (ADMSs) [4]. ADMSs are intended to modernise DNs operation, reduce outages and increase efficiency. However, most DNs are still operated passively. Although they are increasingly incorporating DG units, active DSSE (ADSSE) is not common among utilities [5].

Most utilities use load allocation and load flow analysis for planning purposes [6]. To some extent, these methods can be used to determine the system state. However, load flow analysis is not resilient to erroneous measurements, hence, its results might not always be accurate. Also, it does not incorporate real-time measurements, which is a critical requirement in modern ADNs. Nonetheless, load flow forms a fundamental part of solving SE problems by generating pseudo-measurements and forming the benchmark for state estimation accuracy analysis [7].

In essence, DSSE is not a function in itself; it is an enabling function that supports other operations. Some of the DMS functions facilitated by DSSE include: [8]

- Distribution network observability
- Distribution network controls
- Distribution system asset/equipment optimisation
- Transmission-Distribution coupling interface coordination (e.g. bidirectional power flow control)

- Volt-VAR control
- Power quality management
- Optimal DG units integration and control.
- Microgrid islanding coordination
- Dynamic energy pricing
- Operational forecasting
- Creation of a locational real-time power market

In summary, DSSE is the backbone function of DMS, used to ensure real-time knowledge of the system's operational conditions and its primary application is to improve the network's performance.

1.2 Research motivation

In abidance to the Kyoto protocol [9] in the last 20 years, global interest in smart grids has grown with a vision of a more efficient, reliable, resilient and sustainable electric power system. Renewable energy sources integrated within smart grids are being deployed worldwide to mitigate climate change from greenhouse gas emissions. The incorporation of DG units in distribution networks has transformed them into active systems from their traditional passive mode of operation. The incorporation of DG units requires modern DMS methods for monitoring and controlling the power system.

The IEEE 1547-2003 [10] stipulates standards for interconnections between DG units and the grid to ensure interoperability. The state estimator (SE) is a central functional block in every DMS that predicts the power system's internal state. Therefore, state estimation provides operational visibility that facilitates network automation functions such as fault detection and location, outage management, real-time system monitoring, network security assessment, voltage/reactive power optimisation, energy loss minimisation, generator control, and intelligent load management.

Although the application of state estimation is standard and well researched in transmission systems, its practical application in distribution systems is limited because the operation, design and network topology at the distribution level differ from those of the transmission level as shown in Table 1.2 [11]. The DNs operate at nominal voltages of 132 kV or less, while the transmission networks operate at voltages higher than 132 kV.

Table 1.2: Transmission system's vs Distribution system's characteristics comparison

Transmission systems	**Active Distribution systems**
Meshed topology	Radial topology
Balanced lines and loads	Unbalanced lines and loads
Enough redundancy or observability	Insufficient observability
Low R/X ratio	High R/X ratio

Therefore, the transmission system's state estimation techniques cannot be applied directly to distribution system state estimation. Despite the relatively low adoption of DSSE, it is an essential aspect of active distribution networks.

The accuracy of state estimation depends on the quality and quantity of the state estimator's input. The minimum DSSE requirements are [2]:

1. Up-to-date network model

2. At least a pair of measurement data from each node

    - For example, the real and reactive customer load or voltage magnitude and angle. The pair of measurement data could also be pseudo-measurements that supplement the measured data or aid the detection of bad data in the measurements.

3. Robust telecommunication resources to enable real-time observability

4. An accurate state estimator

It is important for all the inputs to the state estimator to be updated simultaneously to ensure an accurate real-time estimation. Fig. 1.2 shows the state estimator's inputs and outputs.

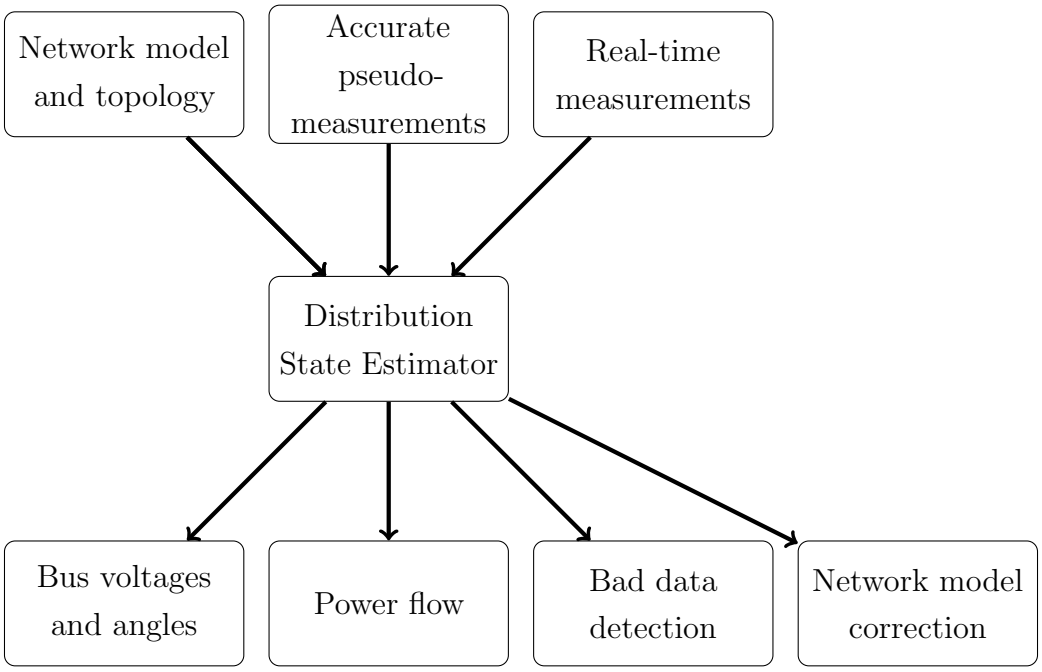

Fig 1.2: DSE inputs and outputs

1.3 Research objectives

Conventional SE approaches are primarily based on the WLS algorithm, which minimizes the total squares of the weighted measurement errors. Nonetheless, with the emergence of smart grids, it is essential to research the suitability of dynamic SE methods that can take advantage of synchrophasor measurements to achieve better precision and real-time SE results. Kalman Filter (KF) methods are recursive/dynamic techniques that reduce error covariance and model the system's state as per its time evolution. However, KF techniques can only be applied to linear models, whereas DNs are nonlinear. Therefore, it is modified KF methods like EKF and Unscented KF that are used for ADSSE. Research by [12] shows that EKF has better estimation than WLS because of its foreknowledge of past predicted results. However, their study only used IEEE data to test the algorithms.

The research objectives of this thesis are:

- Research and implement the WLS and EKF state estimation algorithms on active distribution systems.

- The performances of the algorithms are analysed on modified IEEE 33-bus and IEEE-69

bus test systems, using conventional load flow results as benchmarks.

- The modification of the test system is done through optimal integration of DG units and PMUs using the PSO algorithm.

- Furthermore, real-life data from the ADRES-CONCEPT project will be used to simulate real-life energy consumption and synchrophasor measurements.

.

1.4 Research hypothesis

Active Distribution System State Estimation is difficult because of scarcity of real-time measurement data. The scarcity of measurement data favours the use of dynamic state estimators over static state estimators. Therefore, it is expected that the EKF algorithm which employs linearization of the power flow equations and prior estimation from previous states outperforms the WLS algorithm. Simulation results show that inclusion of PMU and Smart meter data in state estimation improves the quality of the results [13]. EKF is also less sensitive to the amount of PMUs as well as their metrological characteristics according to Macii et al. [14]. As a result, even with fewer and less expensive measurement instruments, low-uncertainty state estimations can be generated using EKF method. Hence, the research hypothesis statement is, *"The EKF algorithm will outperform the WLS approach in active distribution system state estimation when using real-time PMU data."*

1.5 Research questions

The research questions that will enable the achievement of the objectives are;

i. Do dynamic SE techniques(EKF) perform better than static techniques (WLS) on active distribution networks?

ii. Does the incorporation of DG units data affect the accuracy of ADSSE algorithms?

iii. What challenges exist in considering DG units in ADSSE?

iv. Can conventional DSSE algorithms be applied directly to ADSSE without any modification?

1.6 Dissertation outline

The rest of this dissertation is structured as follows:

In Chapter 2, the literature analysis of the state-of-the-art in the DSSE is discussed with respect to developments in the application of the WLS and the EKF algorithms. Other methodologies for DSSE are also discussed. Great focus is placed on the problems posed by the adaptation of transmission system SE approaches to DSSE and the positioning of measurement equipment.

The mathematical problem formulation of the EKF and WLS algorithms is illustrated in Chapter 3. Specifically, it is shown that active grids can only be modelled as nonlinear functions. Active distribution grids are represented by polyphase branch and shunt components whose compound electrical parameters (i.e. impedance / admittance matrices) are symmetrical.

The optimal placement of DG units in distribution grids is demonstrated in Chapter 4. The impacts of the DG units on the grid are also highlighted and the Particle Swarm Optimization (PSO) algorithm used for the optimal placement of the DG units.

Similarly, Chapter 4 presents the IEEE-33 bus and the IEEE-69 bus test systems. First, their models are defined and the results of their load flow are presented. In addition, the ADRES-CONCEPT real-time measurement data used in the experiment are defined.

The results of the deployment of the developed SE methods to the modified test systems are presented in Chapter 5. The performances of the two methods are compared and suggestions on their suitability are also proposed.

Finally, the dissertation is concluded with a summary of the findings in Chapter 6.

1.7 List of publications

As a result of this dissertation research, three conference papers were published:

i. **J. Watitwa** and K. Awodele, "A review on active distribution systems state estimation," in *2019 Southern African Universities Power Engineering Conference/Robotics and Mechatronics/ Pattern Recognition Association of South Africa (SAUPEC/RobMech/ PRASA)* IEEE,2019.

ii. **J. Watitwa** and K. Awodele, "Active Distribution System State Estimation on Modified IEEE-33 bus test system," in *2020 Southern African Universities Power Engineering Conference/Robotics and Mechatronics/ Pattern Recognition Association of South Africa (SAUPEC/RobMech/PRASA)* IEEE,2020.

iii. **J. Watitwa** and K. Awodele, "Active Distribution System State Estimation: Comparison Between Weighted Least Squares and Extended Kalman Filter Algorithms," in *2020 IEEE PES/IAS PowerAfrica*

Chapter 2

Literature Review

State estimation has been an essential application in power system operations and control since its inception by Schweppe [1] in the 1970s. Its research and literature have grown significantly since then. However, most of the applications were focused on high-voltage transmission systems until the early 1990s when pioneering researchers [15–19] considered its integration in distribution systems.

2.1 DSSE implementation challenges

Transmission System SE techniques could not be adopted directly as DSSE methodologies because apart from distribution networks (DNs) featuring fewer measurements and less communication infrastructure, DNs' topology and characteristics are unique as detailed in Table 1.2.

This dissertation includes medium voltage (33kV and 11kV) when referring to DNs, whereas 66kV and above cover sub-transmission and transmission systems. Typically, the power system consists of generators connected to loads via several transmission and distribution lines, running through several substations with monitoring, control and protection devices. The output voltages of the generators are up to 30 kV, so transformers increase the voltage to 132 kV, 400 kV or 765 kV for efficient power transmission and minimise transmission losses [2]. The DNs are generally configured at the receiving end to operate in a weakly meshed or radial configuration of 11 kV up to 33kV.

Beyond the highlighted challenges in Table 1.2, the measurement infrastructure is at the core of state estimation. Even though the pseudo-measurements have less accuracy than real-time data, it is vital to investigate to what extent they should be exploited to supplement available measurements accurately. A pseudo-measurement is a load forecast specific to the load at one node on the network, used in the paradigm of a measurement with a specified error tolerance [20]. The tolerance is generally much higher than that of actual measurement and could be as high as 50% depending on the forecast [20]. In order to increase accuracy in state estimation, the pseudo-measurements are interpolated with higher resolution hourly or sub-hourly data points. Most customer smart meters refresh every 15 minutes.

Load forecasting has been more complicated with the integration of renewable DG units. For instance, PV resources are highly variable; they have fast, intermittent, unpredictable changes. Manitsas et al. [21] show that load allocation and forecasting using historical load data powered by advanced metering infrastructure (AMI) improves the DSSE performance. Generally, AMI equipment (especially PMUs) are expensive, hence their placement in a network needs to be optimised. This research also addresses the optimal placement of PMUs in ADNs.

The DSSE challenges are explained below:

i **High R/X ratios**
The network's resistance (R) to reactance (X) ratio depends mainly on the voltage level and the length of the distribution lines. DNs have significantly low voltage and shorter lines as compared to transmission lines, consequently, they possess higher R/X. High R/X hinders the convergence of iterative algorithms like the Newton-Raphson and de-coupled power flow algorithms [8].

ii **The complexity of the network and unbalanced phases**
DNs usually exist in a radial topology with many nodes. They serve either residential, commercial or industrial customers. Thus, it is common to have single-phase, two-phase or three-phase connections of the feeders. Therefore, the majority of distribution networks are unbalanced. The conventional SE methods assume the existence of a positive sequence and a balanced three-phase system and then evaluate a single-phase equivalent circuit instead. This method cannot be applied in unbalanced circuits as in DNs.

Each phase of an unbalanced network has to be analysed individually. A three-phase

system has triple the number of state variables as a single-phase equivalent network. Thus, the complexity of the SE problem is increased, and higher computing power will be needed to solve unbalanced three-phase circuits. To reduce the complexity and computing power requirements, the distribution network operators opt for topology simplification and parallel computing, respectively [22].

iii **Limited availability of real-time data.**
Traditionally, distribution networks have been operated passively- i.e. the distribution control centres had minimal real-time visibility of the network. Most distribution networks only have metering up to the substation level. The network is therefore under-observed or partially observable as compared to transmission systems, which are over-determined by redundant measurements.

Conventional SE methods work on the principle of an over-observed network. Therefore, several authors have attempted to replicate this scenario in DSSE by generating pseudo measurements from stochastic load data. Unfortunately, the large proportions of pseudo measurements in DSSE compromise its precision [23].

However, by taking advantage of new technologies like artificial intelligence (AI), machine learning, and AMI, some authors have proposed intelligent load estimation techniques. References [24–26] investigated the inclusion of smart meter measurement in DSSE for load estimation to increase accuracy.

Table 2.1 summarises the ADSSE challenges:

2.2 DSSE methodologies

2.2.1 Adaption of TSSE methods into DSSE

Pioneering DSSE researchers attempted to adapt state estimation techniques designed for transmission systems into distribution systems. WLS is the most common state estimation algorithm. It has been extensively used in its original form and adapted with improvements to make it robust. Its mathematical formulation is explained in Chapter 4

Sakis and Zhang [27] described a multiphase power flow analysis based on Newton Raphson's method. Despite the method performing well, it did not consider distributed loads along

Table 2.1: Summary of challenges in the implementation of DSSE

Challenge	Summary
Observability	• Observability is the biggest challenge in the implementation of ADSSE. • Measurement equipment are usually rarely located in a sufficient number of DN nodes. • Lack of observability necessitates the use of pseudo-measurements.
Telecommunication infrastructure	• Measurement data must be relayed to data collection centers in real time. • The incorporation of AMI data from different sources requires synchronization before updating the state estimator, which increases the infrastructure requirements.
Network complexity	• DNs have several nodes- up to 10000. • The phases of the DNs are unbalanced, which merits three-phase ADSSE modelling, thus increasing the complexity of the SE process and the need for higher computing power.
Line parameters	• The DNs have a high R/X that can impede the convergence of the ADSSE algorithm.
Uncertainty in network parameters and topology	• The topology and parameters of DNs are largely under-reported due to limited monitoring. • Versatile rate of change due to the incorporation of DG units.

with distribution circuits. Thereafter, they [28] employed synchronised measurements in an asymmetric model of a DNs and proposed a decoupled multi-phase state estimator. The distributed load was successfully modelled and estimated as the load current.

Lu et al. [17] proposed a three-phase DSSE algorithm, where they used the WLS method to compute the real-time states of distribution systems modelled by their actual three phases. Additionally, they introduced a rectangular form SE based on current instead of power since the current method can handle more types of measurements. The test results showed that the current based formulation is suitable for DSSE.

Stevens et al. [29] analysed the performance of conventional power flow routines for real-time distribution automation applications. They compared Gauss-Seidel and Newton-Raphson methods for power flow calculations of radial circuits and weakly meshed topology to determine their efficiency in DSSE. The Newton-Raphson emerged as the most suitable method however, its memory and computational requirements are excessive for real-time analysis of complex radial circuits.

A three-phase fast decoupled SE is presented in [30], where the gain matrix is kept constant and symmetric to reduce the computational time. However, this method lacks the robustness to handle bad data.

2.3 Measurement equipment placement, accuracy, and network observability

Distribution networks have many nodes, and it is uneconomical to have meters at every node. However, redundant SE requires twice as many measurements as variables to ensure observability. Therefore, much research has gone into the optimal placement of measuring equipment in the grid to achieve system-wide observability with as minimal real-time measurements as possible, coupled with pseudo-measurements and virtual measurements. PMUs have been extensively used in transmission systems, and sufficient research is targeted to realise their benefits in distribution systems as well.

Some works that focus on optimal measurement placement to improve observability and accuracy in SE results are [31], [32], [33], [34], [35], [36]. Similarly, Kahunzire and Awodele. [4] and Li et al. [37]considered the effect of PMU placement in Distributed Networks to improve DSSE speed and accuracy. PMUs can measure both the magnitude and angle of the voltage as well as the line current and its angle.

Liu et al. [38] investigated the trade-offs between the deployment of smart meters and PMUs. They aimed to find the optimal measurement infrastructure in active distribution systems while minimising the investment cost. They established that smart meters with optimized placement can help to meet the same required accuracy limits as PMUs at a lower cost. Subsequently, Singh et al. [39] described a framework of meter placement. The proposed method divided the grid geometrically according to the measurement error variance and used a non-iterative method to seek areas with high variances as the potential location of

the meters. The method reduces the voltage and angle errors by determining the minimum voltage magnitude and power measurements necessary for accurate DSSE.

The WLS method is highly dependent on the accuracy of the measurements fed into the state estimator and assigns weights proportional to the measurement accuracy. Virtual measurements, e.g. the slack bus assigned at 1 per unit and zero degrees, get the highest weight, followed by real measurements while pseudo-measurements are assigned weights as low as 50% due to their high uncertainty. Li et al. [37] modelled a three-phase DSSE that considers customer's real and estimated load measurements as expected values with errors. The stochastic results show that the estimated deviation of the system state is affected by the load error correlation, real-time measurement availability, load estimate errors and measurement placement.

2.3.1 Incorporating measurements of different timescales in state estimation.

Distribution systems typically have less advanced measurement infrastructure than transmission systems. Initially, metering was done up to the substation level using remote terminal units (RTUs) and SCADA. However, recent developments have seen the integration of PMUs in distribution networks. PMU measurements are synchronized to the global position system (GPS). Hence their resolution is in tenths of seconds, while the SCADA signals are in tens of seconds. The addition of smart meters, which are only telemetered after every 15 minutes makes it necessary to ensure synchronisation of the out-of-sync measurements before they are fed into a state estimator.

Various scholars have researched on integrating various timescale measurements, such as smart meter data and PMU data concurrently:

Gómez-Expósito et al. [40] considered the different refreshing rates of higher resolution SCADA and lower resolution smart meter measurements and structured a state estimation model in the two-time scales. Their model integrates pseudo-measurements derived from AMI data with real-time SCADA measurements. Pseudo-measurements are not measurements, but they are treated as such in the state-estimation algorithm. If more accurate pseudo-measurements are used, they will improve the precision of state estimate.

Smart meters sample their data in an unsynchronised manner. Alimardani et al. [41] stated

that load varies typically through a short period and then proposed a DSSE method that adjusts the smart meter's error variance and means to modify its weight as a function of its resolution.

Han et al. [42] analysed the advantage of using different real-time measurements in DSSE and to what extent integrated data can improve the results. They found that increasing the number of meters or type of measurements increases the accuracy. A hybrid SE method was developed to handle multiple input sources. The paper, together with [43, 44] are valuable resources in analysing the effects of redundancy and sampling of unsynchronised measurements in DSSE.

Ideally, when incorporating measurements with different resolutions, one can either make an estimate at the resolution of the lowest frequency of the measurements or at a higher resolution by incorporating older and out-of-sync measurements. Older measurements, however, have less relevance in real-time SE and may introduce inaccuracies as they will be post-dated.

Distribution systems are mostly unobservable if only the real-time measurements are used. Utilities use load forecasting to supplement the actual measurements. The pseudo-measurements are modelled as normally distributed variables with known mean and variance because the WLS and EKF methods are only compatible with Gaussian distributed inputs. Singh et al. [45], [46] used customer loads presented in a Gaussian mixture model as pseudo-measurements in DSSE.

Ideally, a probabilistic load model based on historical load data and customers' billing information is used to model the pseudo-measurements [47]. Since pseudo-measurements are predicted and estimated values, they have a lower confidence weight (+-50%) than actual measurements.Wu et al. [48] believe that adding pseudo-measurements might not necessarily improve SE accuracy but only ensure network observability. Therefore, pseudo-measurements can only be used to increase measurement redundancy to improve observability and not bad data detection since they do not represent the current state of the system. However, just enough forecasted data must be added to the state estimator inputs to ensure the bare-minimum redundancy as too many pseudo-measurements will affect the results negatively since the results will be highly associated with their low weights [20].

2.3.2 Advanced metering infrastructure

Smart meter deployment at the consumer level is a modern trend. By the end of 2016, 2.9 million, 70 million and 96 million had been installed in the UK, the US and China, respectively [49]. Mostly, the meters are used for basic meter-reading and billing purposes by the utilities. However, advanced metering infrastructure (AMI) data can be extended to DSSE usage either through incorporation directly as state estimator inputs or used for load forecasting and pseudo-measurement generation. Incorporating smart meter data directly into the estimator could be the best-case scenario but there are a few challenges that hinder this. First, most smart meters currently only have a resolution of 15 minutes, therefore, real-time state estimation cannot be achieved. Second, the telecommunication infrastructure available cannot process, store and transmit the data immeadiately to the data concentrators. Most utilities only relay the collected data every 24 hours [50]. Further, there are privacy issues regarding the use of customer data, and not all consumers have signed off their data being used by carriers. Therefore, smart meter data is normally used for forecasting applications as discussed by the following authors.

Baran et al. [24] converted the voltage and consumer power demand readings into branch currents and then used the readings as both pseudo-measurements and real-time measurements. The comparison of the two cases shows that the errors in the DSSE results decrease with additional data through AMI. References [51, 52] also used the same approach and came to the same conclusion.

Wang et al. [49] provided a comprehensive review of smart meter data analytics in retail markets, including its application in load forecasting, fault detection, and demand response. The authors also highlight future research areas in smart meter big data analytics and machine learning technologies.

2.4 Topology identification

The distribution system's network topology is more complex than the transmission system's. Although the distribution transformer's on-load tap changers are assumed to be at a fixed position throughout, the status of other switches and circuit breakers keep changing due to the dynamic nature of distribution systems. However, most utilities still operate their distribution networks passively and only react to contingent emergencies. Nonetheless, the state estimator needs an accurate assumption of the network's current state to base its calculations on. Therefore, a distribution network topology processor is essential. It identifies the network's

configuration from its network connectivity model and dynamic switch status [53] just like in transmission systems.

The network parameters that constitute a distribution system's topology include [2]:

- Line parameters, e.g. line reactance and resistance
- Bus parameters like the number of connected customers, power system equipment, and respective shunt parameters
- Network connectivity or statuses of the switch positions
- The specific equipment ratings, e.g. transformer or circuit breaker ratings

If the above parameters are unreported in real-time, the topology processor will create a simplified network model with just the necessary information for state estimation. Reference [2] gives a clear overview of power system parameter estimation and bad data detection. Some authors who have specially handled topology identification of distribution networks attempted to take advantage of modern technology such as micro-PMUs combined with GIS (geographic information system) [54], [55]. Micro-PMUs are smaller, less expensive, and designed explicitly for distribution networks. For instance, Disfani et al. [56] developed a network separation algorithm that includes micro-PMUs in smaller sub-networks to mitigate the effects of noise in large networks.

2.5 Bad data detection and identification

Ideally, the measurement infrastructure should have zero error, but this cannot ever be the case. Therefore, the state estimator inputs and results always contain some errors. Bad data detection and identification is the process in which the state estimator detects erroneous measurements by looking at the difference between the measured data and the estimated variables, and deciding whether it is within the threshold. Two of the conventional bad data detection and identification methods are the chi-square test and the normalised residual test. In the chi-squares test, the total system error is compared to a realistic threshold, while the latter method, analyses the difference between the measurement and state variable. The normalised residual test is more accurate than chi-squares [2].

On discovery of incorrect measurements, they should be removed. The error with the most significant residual is removed first; then, the state estimation is rerun. This process is repeated until no bad data is detected. However, if some of the measurement errors are correlated, this approach might fail to converge. In which case, the hypothesis testing approach is more suitable [57]. Also, the problem can be complex as network size increases and the method might not detect multiple correlated errors [58].

Van Cutsem et al. [59] and Wu et al. [60] carried out some of the pioneering studies in bad data detection in transmission lines in the late 80s and their studies can equally be employed in DSSE. Similarly, Chen et al. [61] took advantage of the relationship between bad data detection as a function of the state estimator and measurement redundancy. They noted that bad data appearing in critical measurements cannot be detected. Hence, the critical measurements can be transformed into redundant measurements by optimal placement of PMUs in the distribution network, which improves the state estimator's bad data detection and identification capability. Mutanen et al. [62] investigated the use of pseudo-measurements for bad data detection to limited success and concluded that pseudo-measurements do not reflect the current state of the system, and should therefore not be used to increase redundancy.

Fig. 2.1 represents the operational flow chart of DSSE functions.

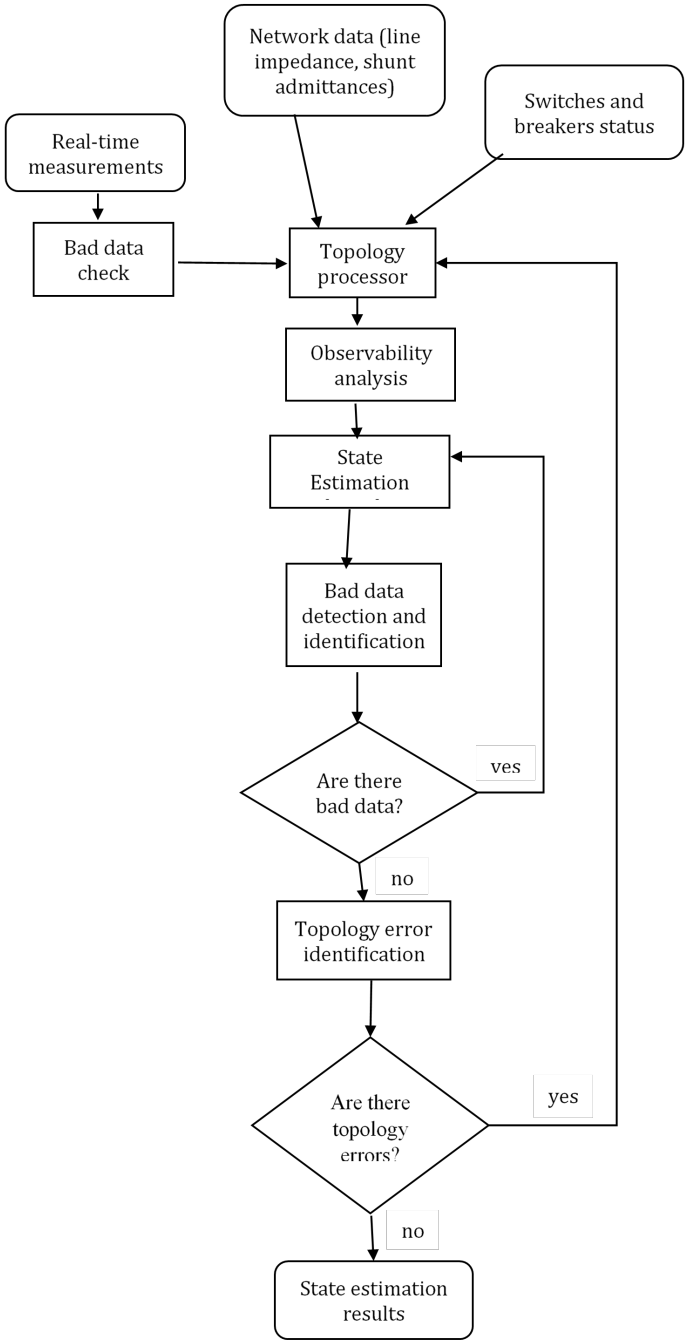

Figure 2.1: Operational flow chart of DSSE functions [2]

2.6 Challenges in real-time DSSE implementation on actual utility grids

In as much as DSSE research has shown progress in synthetic test grids, the main aim is to achieve feasibility in actual utility grids. Apart from the already mentioned challenges like low redundancy and unbalanced systems, there are several other difficulties identified by several authors:

Atanackovic et al. [63] deployed and tuned real-time DSSE at the BC Hydro control centre to enable real-time power system monitoring and control. However, they found out that one of the most challenging tasks was the tuning of measurement weights. Although other activities, such as network model corrections and load flow tuning, often took a lot of time and detailed analysis, they were fairly routine once the DSSE process was set up. On the other hand, tuning measurement weights was iterative and needed to be carried out repeatedly.

Gonzalez et al. [64] show a practical implementation of a state estimator for distribution systems in the context of the Spanish pilot project PRICE-GDI. They presented an improved accuracy level in the results when pseudo-measurements were incorporated in the DSSE. However, the pseudo-measurements had to be calculated from load measurements with at least an hourly resolution.

Pignati et al. [65] described the Ecole Polytechnique Federale de Lausanne's (EPFL's) smart grid real-time monitoring system and experimentally tested the idea of a 20 kV active distribution network real-time state estimation. They then built and implemented the entire infrastructure consisting of dedicated PMUs linked to the medium-voltage side of the network, a dedicated communication network and an advanced state-of-the-art SE method that combines phasor-data concentration and state-of-the-art estimation processes. Special care was taken to make the whole chain resilient to cyber threats, equipment failures and power outages. The latency reached was within 65ms. The average refresh rate was 20ms. Their research confirmed the real-time realization of DSSE.

One of the challenging tasks related to the real-time control of modern power systems is the development of a fast state estimation method. The use of PMUs, which are structured to provide time-synchronized measurements with low latency, is helpful in addressing this challenge. However, the use of PMUs often accumulates delays due to the processes shown in Fig. 2.2 and elaborated below [66]:

- **Synchrophasor estimation:** PMUs need a finite window length to infer the calculation before they submit it.

- **Telecommunication:** the transmission feature of the calculated values over the telecommunications channels often has some latency.

- **Measurement concentration** at the phasor data concentrator (PDC) and collection of data from the PDC.

- The state estimation algorithm itself.

All of these processes are chronological and thus accumulate a delay of around 60-80ms.

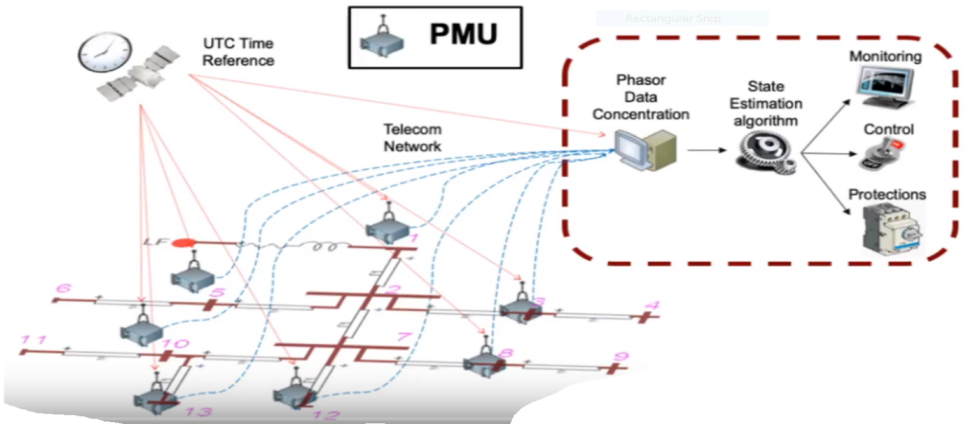

Figure 2.2: Typical distribution system state estimation architecture with PMUs [66]

2.7 Classification of DSSE Algorithms

Previous sections discussed the context and broad theory of the DSSE. This section will cover the specific SE algorithms used to solve the problem. SE uses a variety of methods and algorithms to determine the most likely state of the system based on the available measurements.

SE algorithms are categorized as either static algorithms or recursive algorithms. Static state estimators only record inputs at a given point in time, and similarly, the output of the SE is at the same time (t). Recursive algorithms compensate for dynamic knowledge and forecast the future estimates. The WLS algorithm has been more popular than KF for a long time,

due to its low SE refresh rate. However, the prospect of substantially raising the SE refresh rate of the KF algorithm using synchrophasor measurements has led to a reconsideration of its efficacy. This work will concentrate on the methods of WLS and EKF.

2.7.1 Static DSSE

Static DSSE assumes that the power system state is not changing between consecutive state updates. It has three aspects:

i **The choice of state variables:** different authors [19, 67, 68] have either chosen the nodal voltage or the branch-current. The branch-current offers better computational efficiency and reduces sensitivity to network parameters. Further discussion on this is in subsection 2.7.2.

ii **The choice of the state estimator:** several studies have concluded that the WLS is the most suitable estimator for DSSE because it has low redundancy levels. Singh et al. [69] investigated the WLS, Weighted Least Absolute Value (WLAV) and Schweppe-type Huber generalised maximum-likelihood (SHGM) estimators and concluded that the methodology of WLAV and SHGM need significant modifications to obtain consistent and accurate estimates. On the other hand, WLS gave consistent and better-quality performance when applied to distribution systems. Hence, WLS is a suitable solver for the DSSE problem.

iii **Measurement configuration and observability issues:** a significant DSSE challenges is optimal placement measurement points across the numerous available nodes. Previous experiments have used a load estimation procedure based on historical consumption data to formulate pseudo-measurements. Meanwhile, high dependence on pseudo-measurements lowers the quality of the state estimates. Substantial research [39] has gone into establishing optimal meter placement techniques to guarantee observability at economical costs.

Fig.2.3 illustrates static SE process.

2.7.2 Choosing either the branch-current or the nodal voltage as the state variable

The choice of the state variable to use (either voltage or current) was a key decision in the initial DSSE techniques. The branch-current SE (BCSE) applies the branch-currents as the state variables, whereas the node-voltage-based state estimation (NVSE) considers the node

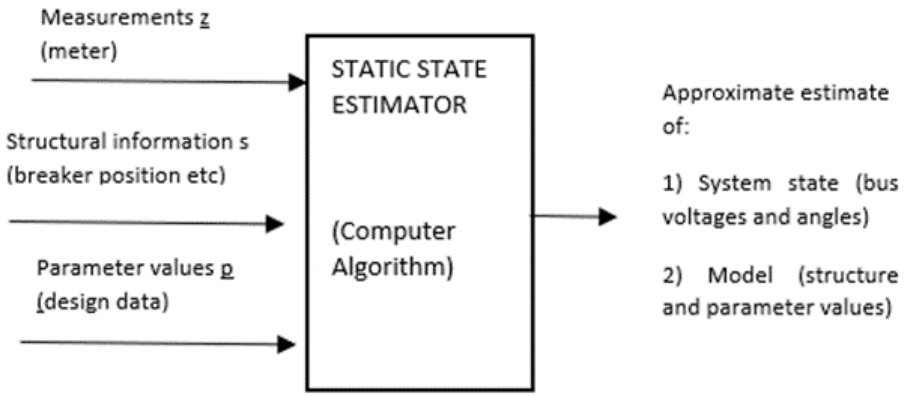

Figure 2.3: Illustration of static state estimation [70]

voltages as the state variables. Mesut and Kelley [19] initiated research in BCSE and noted that it was superior to NVSE in terms of computational speed and memory requirements. The branch current method suits weakly meshed and radial networks since it is insensitive to line parameters and it improves convergence and bad data handling. Improved variations of the BCSE technique are presented in [67, 71, 72].

Pau et al. [73] compared BCSE and NVSE on the basis of accuracy and efficiency between BCSE and NVSE. By using an expanded version that requires a slack bus voltage in the state vector, the results show that BCSE is more reliable. More comparisons are summarised in [8] as shown in Table 2.2. Baran, et al. [74] included voltage magnitude measurements in BCSE and showed that this improved the accuracy of the results further.

Table 2.2 displays a comparison between BCSE and NVSE

Table 2.2: Comparison between branch-current and nodal voltage as choice of state variable in state estimation [11]

Property	**BCSE**	**NVSE**
Implementation	Simple	Complex
PMUs inclusion	Voltage phasor: complex Current phasor: simple	Voltage phasor: simple Current phasor: complex
Computational time	Less	More
Numerical Stability (Sensitivity to measurement weights)	No	Yes
Convergence	Good	May not converge if ill-conditioned
Sensitivity to three-phase power base variation	No	Yes
Phase decoupling	Yes	No

2.7.3 Recursive DSSE

Unlike static DSSE, where loads are modeled as constants, recursive DSSE considers evolving smart grid technologies such as DGs, electric vehicles (EVs), intelligent electronic devices (IEDs) and demand-side management (DMS). The accuracy of load modeling directly affects the control, operation, simulation and analysis of power systems. For example, the accuracy of the SE function is affected by the load parameters. As a consequence, the existence of parameter errors in load modeling can lead to inaccurate estimates. Dynamic load modeling surveys were developed and introduced in 1995 [75, 76]. More recent work include [77, 78].

Conventional SE approaches were mostly static and based heavily on transmission systems [79–82] since the key source of power was hydro and steam turbines that followed predictable and sluggish patterns. Nevertheless, with the emergence of distributed energy resources (DER) and the introduction of PMUs and smart meters at the distribution level, the need for complex SE has become evident. The distinction between static and dynamic SE is that static SE assumes that the state variable is in a stable or quasi-permanent state (constant with respect to time). On the other hand, the variable in dynamic SE varies with time [83]. Static DSSE results from the further simplification of the transmission systems' SE, which totally ignores the state transfer information and instead retains the nonlinear (Gaussian

distributed) measurement function. Therefore, the static DSSE does not have a memory of the states at the previous time steps [1], while dynamic DSSE typically consists of two steps (a priori and aposteri) i.e. a prediction and an estimation step.

Kalman Filter(KF) [84, 85] is the primary dynamic state estimation form. There are several variants of the KF system. The Discrete Kalman Filter (DKF) is used for linear systems, while the EKF and the Iterated Kalman Filter (IKF) are used for non-linear systems. The DKF is the only pure KF method of the three because it is the only exact version of the original KF algorithm.

In the KF method, the measurement function must be represented as a linear function. Active DNs are, however, modelled as nonlinear equations, which means that the KF method cannot be used in Active Distribution Systems State Estimation (ADSSE). As a consequence, nonlinear KF methods such as EKF, Unscented KF (UKF), IKF or Ensemble KF (EnKF) should be used [12]. Studies by [12, 86, 87] show that complex SE techniques typically outperform WLS. Their work, however, did not consider the inclusion of DG Units.

Although recursive techniques can provide almost real-time monitoring, they are not commonly implemented in DNs because; they require high-quality resolution measurements from IEDs such as PMUs, which are still not widely installed in DNs [68], and distribution networks are typically large, requiring high computational speeds. References [88–90] provide a detailed literature survey on recursive SE.

2.7.4 Kalman Filter applications in Power System State Estimation

This section presents some of the applications of the KF algorithm in PSSE since its inception in the 1960s. R. Kalman [85] first proposed the KF state estimation and linear filtering for the study of dynamic systems. The approach has gained a great deal of popularity in other technology fields, but its application to power systems has been limited due to its sophistication including [66]:

- the need for a process model that requires the specification of many parameters;
- the development of complementary applications is getting more difficult, e.g. a bad-data processor must take into account that a significant residual may be attributed not only to a calculation error, but also to a sudden change in the process model;

- higher computational time does not make real-time execution simpler.

While the KF algorithm can have an estimation precision better than the WLS, its adoption has been minimal. Some of the authors that dedicated their work to it include:

Debs et al. [91] proposed a standard application of the Kalman-Bucy linear estimation theory, resulting in the tracking state estimator in power systems. However, the authors carried out simulations on a linear DC load flow model. These findings cannot be extrapolated to the real AC load flow case without actual experiments. Nevertheless, their work promoted the idea that the tracking state estimator is a good approach to state estimation for power systems.

Nishiya et al. [92] presented the EKF algorithm, a non-linear variant of the KF. The EKF algorithm discriminates between the occurrence of bad data, changes in network architecture and sudden state variations.

A more recent comparative study [93] shows that the Ensemble Kalman Filter (EnKF) algorithm can achieve relatively good estimation precision without relying on the measurement interpolation process by using a limited number of samples. This result reveals that, when using the measurement covariance, EnKF is more robust than EKF and Unscented Kalman Filter (UKF) at a lower sampling rate. Nevertheless, the EKF and UKF have a lower processing time than the EnKF, which is often more prone to outliers.

Sarri et al. [94] compared the output of WLS and the Itirated Kalman Filter (IKF) algorithm and showed that IKF performed better. The paper also showed that the efficiency of WLS and IKF techniques relies on the calculation and the processing of covariance matrices. The measurement covariance matrix calculates how much the IKF trusts the measurements while the process covariance matrix weight how much the IKF algorithm trusts the estimated values.

Another of the pioneering work in dynamic state estimation is [95], where a decoupled recursive algorithm was used to separately measure the bus voltage magnitude and the voltage angle. However, this proposal underestimated the influence of voltage magnitude and angle estimation noise and was equally computationally inefficient. Similarly, a recent development in recursive SE is discussed in [96], which proposed an UKF algorithm.

Gelagaev et al. [97] compared WLS and EKF using the modified 34-bus IEEE test feeder and observed that the EKF required less iteration and computation time. They generated the input measurements by ladder iterative technique. The downside of the EKF is that it requires some previous knowledge of the states. The main difference between their research and this dissertation is that this dissertation uses real-time data.

2.8 Summary

This dissertation compares the efficiency of WLS and EKF on ADNs by using PMU data and real-time load measurements. The dissertation's contributions can be summarized as follows:

- From the literature reviewed on distribution systems state estimation, most of the work is based on adaptation of transmission system state estimation methods on passive distribution systems. The issue of measurement insufficiency is addressed using pseudo-measurements. However, the issue of including Distributed Generators and real-time PMU measurements is only addressed by Zanni et al. [66]. This dissertation explores existing WLS and EKF state estimation methods and evaluates their applicability to the active distribution networks. The chosen algorithms are benchmarked against the Newton Raphson's load flow results of the test systems.

- Regarding the DG and PMU units placement, this dissertation uses the Particle Swarm Optimization technique. The PMU readings are intended to improve the quality of the state estimation results. The PSO is a population-based optimization method inspired by flocking birds' social behaviour. It randomly generates the initial population, and then the generated particles move towards the optimal solution. Incorporation of the DG units improves the voltage profile of the test systems and reduces their active power losses.

Chapter 3

Optimization of Distributed Generation Units Sizing and Placement

This study modifies the existing IEEE- 33 bus and the IEEE-69 bus test systems to include DG units, making them active distribution systems. DGs are classified as small generators connected in close proximity to consumers. The integration of DGs in distribution networks is the primary driver towards next-generation smart grids. The installation of DGs worldwide has become popular due to their low investment costs, low power losses, advances in policies to curb global warming, and regulations favouring private sector participation in electricity generation and distribution. Consumers are having a rising interest in installing independent power plants to not only satisfy their demand but also sell excess power to the grid for an extra income. However, this creates new challenges in distribution systems, which were designed initially as passive systems with minimal operational interactions. Therefore, the DSOs and DG owners need to update their operational strategies to accommodate the new changes equally.

3.1 Impacts of DG on Active Distribution Systems Modelling

Theoretically, DG incorporation should improve power quality, voltage profile, reduce power system congestion, and improve the security of supply. However, in reality, the integration of DGs into DNs has created some technical challenges, such as voltage rise and reverse power flow. The unique characteristics of DNs (radial topology, high R/X, unbalance and imperfect observability), coupled with the fluctuating output of renewable DG make it even more challenging to simulate active distribution system state estimation on existing test systems due to the following reasons [98]:

i It is difficult to predict renewable DG power production because it depends on the weather. For example, wind speed directly affects the generation of wind turbine generators. Since it is hard to predict the wind speed at a given time accurately, there would be inevitable forecasting errors.

ii Reverse power flow: When the output of the DGs that are coupled with the main utility exceeds the demand at the point of coupling, there will be a reverse power flow to the grid.

iii The topology of DNs is normally undetermined at low voltage levels. The uncertainty of the output of the DGs further accelerates the frequency of change in the network topology. For instance, the converters and inverters in PV installations need to be monitored and regularly switched depending on the irradiation received.

iv Undetermined state at DG installation points: Real-time measurement devices are limited by their ability to communicate their recordings to the control centre. In this regard, the default refresh rates of the current SCADA-PSSE processes are of the order of a few minutes, while the application time frames of real-time measurement devices are between few hundreds of milliseconds to a few seconds [65].

The integration of DGs into DNs has significant effects on the electricity market. If the DGs generate more power than is required to meet the DG's demand, they are liable to sell the surplus to the utility companies. The DSOs must therefore carefully consider the uncertainty of the DGs to guarantee that the supply-demand balance will be retained before signing a power purchase agreement with the owners. The conventional top-down, centralised

energy market practices are slowly evolving into decentralised markets, which facilitate better interactions between the DSOs, prosumers, and consumers.

3.2 Modelling Approaches for Test Systems with DG

Various methodologies for load modelling with DG uncertainty have been investigated in [99]. Different test models, analytical and simulation tools for passive electric distribution system analysis have existed for a while. These tools are generally simple, just enough for basic bench-marking and comparative studies in research and academia. With recent advances in computer technology and increase in power system complexity, the amount of system data collected is significant, and control algorithms need to be versatile to satisfy practical engineering analysis and applications. Accordingly, distribution test systems must be modelled to appropriately represent ADNs.

The IEEE-33 bus and IEEE-69 bus test systems were selected for this research since they have standardised complex parameters, and network topology, and precise data on geographic distribution, nodal connections, and load profile. They are modified to include DGs.

3.3 Optimal Sizing and Placement of DGs Using PSO

Appropriate DG placement reduces the system's losses and improves the voltage profile. Various techniques have been applied for optimal sizing and placement of multiple DGs in DNs, including genetic algorithm (GA), particle swarm optimization (PSO), taboo search, and other various hybrid methods [100], [101], [102].

The PSO is a population-based optimization method, inspired by the social behaviour of birds flocking. It randomly generates the initial population, and then the generated particles move towards the optimal solution [103]. During the flight, each bird adjusts its position as per its own experience (P_{best}) and its neighbours (G_{best}) to achieve a global minimum (or maximum). Thus, the DG active power and location are considered as particles, and the optimal solution is established by iteratively solving (3.1) and (3.2).

$$V_{id}^{n+1} = V_{id}^{n} + c_1 r_1 (P_{best} b_{id}^{n} - x_{id}^{n}) + c_2 r_2 (G_{best} b_{id}^{n} - x_{id}^{n}) \tag{3.1}$$

$$x_{id}^{n+1} = x_{id}^{n} + V_{id}^{n+1} \tag{3.2}$$

where; x_{id} and V_{id} are the position and velocity of the particle; c_1 and c_2 are the acceleration constants (either with a value of 1 or 2); and r_1 and r_2 are two random values ranging from 0 to 1.

The PSO procedure is illustrated in Fig. 3.1.

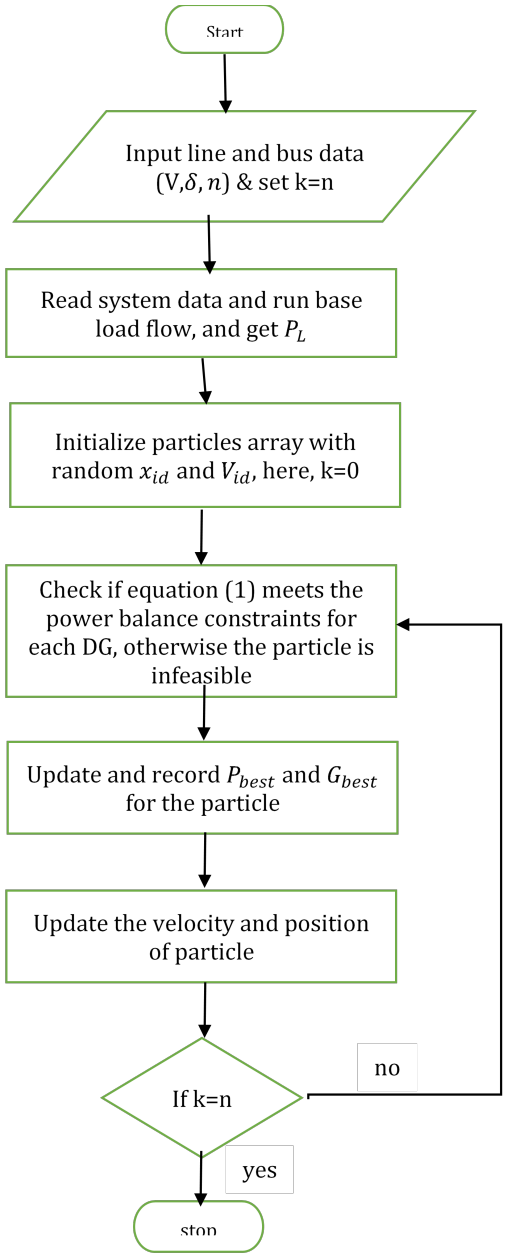

Figure 3.1: Flowchart for optimal DG sizing and placement using PSO algorithm

The active power loss of the entire distribution system is considered as the problem constraint.

The loss in the system is calculated as shown in (3.3) [103].

$$P_L = \sum_{i=1}^{N} \sum_{i=1}^{N} A_{ij}(P_i P_j + Q_i Q_j) + B_{ij}(Q_i P_j + P_i Q_j) \tag{3.3}$$

where,

$$A_{ij} = \frac{R_{ij} \cos(\delta_i - \delta_j)}{V_i V_j} \tag{3.4}$$

$$B_{ij} = \frac{R_{ij} \sin(\delta_i - \delta_j)}{V_i V_j} \tag{3.5}$$

and: P_i and Q_i are the net real and reactive power injections at bus i respectively, and R_{ij} is the resistance of line $i-j$ between bus i and bus j. V_i and δ_i are the voltage magnitude and angle at bus i respectively.

The objective of the PSO technique is to minimize the total real power loss as illustrated by equations (3.6)-(3.9);

$$\text{Minimize} \quad P_L = \sum_{k}^{N} LOSS_k \tag{3.6}$$

Subject to power balance constraints

$$\sum_{i=1}^{N} P_{DGi} = \sum_{i=1}^{N} P_{Di} + P_L \tag{3.7}$$

where: $LOSS_k$ is the loss at bus k, N is the total number of buses, P_L is the active power loss in the distribution system, P_{DGi} is the active power generation from the DG unit at bus i, and P_{Di} is the power demand at the bus i. Therefore, the minimum loss equation at bus i becomes;

$$P_i = P_{DGi} - P_{Di} = -\frac{1}{A_{ii}} \sum_{j \neq i}^{n} (A_{ij} P_j - B_{ij} Q_j) \tag{3.8}$$

Hence,

$$P_{DGi} = P_{Di} - \frac{1}{A_{ii}} \sum_{j \neq i}^{n} (A_{ij} P_j - B_{ij} Q_j) \tag{3.9}$$

Equation (3.9) gives the optimal DG size for minimum total active power loss.

3.4 IEEE 33-Bus Test system description

The IEEE 33-bus test system (Figure 3.2) was modified to include DG units. The system is 12.66 kV with a 2-feeder substation and 33 buses. The total load active and reactive power are 3715 kW and 2300 kVar respectively [104].

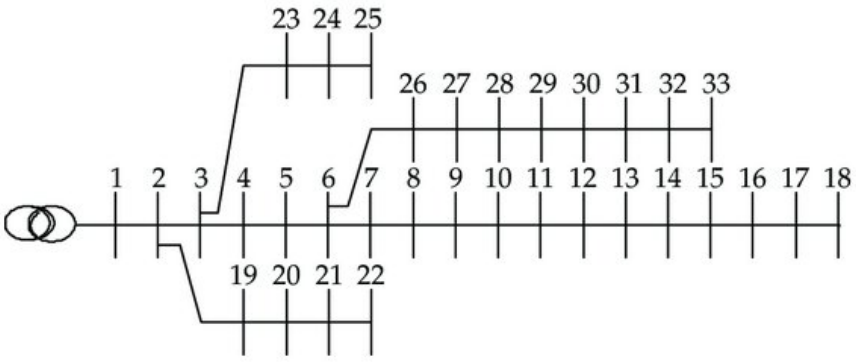

Figure 3.2: Single-line diagram of the IEEE 33-bus test system

3.4.1 Load flow results

Load flow analysis of a power system yields voltage magnitudes and phase angles at its buses, and power flows through its lines. Gauss-Seidel, Newton-Raphson, and fast decoupled methods are the conventional numerical methods for load flow analysis. In the optimization problem in this research, the load flow subroutine was executed in MATLAB [105] using the Newton-Raphson method. Equations (3.10) and (3.11) were used to compute the real and reactive power injections at the buses of the test system.

$$P_i = P_{DGi} - P_{Di} = |V_i| \sum |V_k|(G_{ik}\cos(\theta_i - \theta_k) + B_{ik}\sin(\theta_i - \theta_k)) \tag{3.10}$$

$$Q_i = Q_{DGi} - Q_{Di} = |V_i| \sum |V_k|(G_{ik}\sin(\theta_i - \theta_k) + B_{ik}\cos(\theta_i - \theta_k \tag{3.11}$$

Where; P_i and Q_i are the active power in MW, reactive power in MVar, P_{DGi}, and Q_{DGi} are the DG's active and reactive power at bus i respectively. P_{Di} and Q_{Di} are the active and reactive loads at bus i. V_k and V_i are the per unit voltage magnitudes at bus k and i

respectively. G_{ik} and B_{ik} are the real and the imaginary parts of the i^{th} row and k^{th} column of the bus admittance matrix. θ_i and θ_k are the voltage phase angles at the respective buses.

The system's line and load data are the inputs into the Newton-Raphson algorithm while the nodal voltage magnitudes and total power losses are outputs. The PSO uses these results to determine the optimal location of the DG. A second execution of the load flow subroutine yields the required variables after DG inclusion. Table 3.1 shows a summary of the load flow results without DG inclusion.

Table 3.1: IEEE-33 bus load flow results

	P(Active Power) kW	Q(Reactive Power) kVar
Total generation	3996.59	2487.96
Total PQ load	3715	2300
Total losses	272	178.06

3.4.2 Optimal DG placement in the IEEE 33-bus test system.

The PSO algorithm (Figure 3.1) is executed for optimal DG placement to reduce the real power losses and to improve the voltage profile. It is presumed that only Solar Photovoltaic (PV) DG units are integrated. A 2590.9 kW DG was installed on bus 6. Figure 3.3 shows the voltage magnitudes before and after DG placement. The voltage profile improved to within 0.94 to 1 p.u with optimal DG placement, from 0.88 to 1.02 p.u without DG units in the system. In turn, the overall power loss decreased to 111 kW from 272 KW.

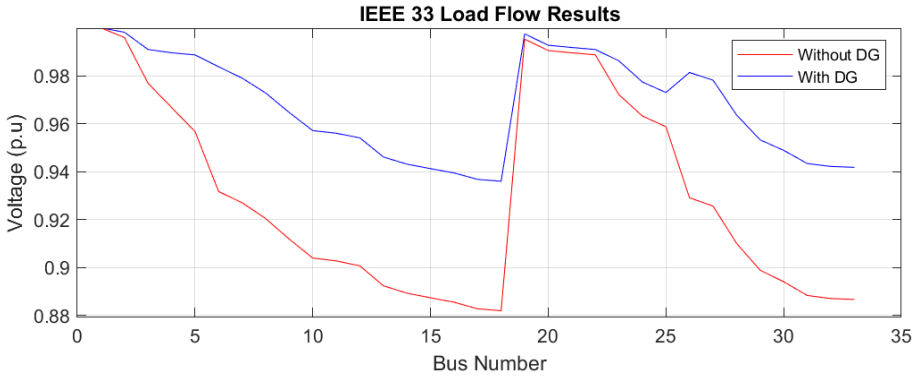

Figure 3.3: IEEE 33-bus test system's voltage profile before and after DG unit placement

The PSO pseudo-code for finding DG's optimal size and location to minimize the real power loss is as follows [106]:

- Step 1: Create a random population (array) of particles with random positions and velocities on dimensions in the solution space. Make the iteration counter k equal to zero.

- Step 2: Calculate the total real power loss for each particle if the bus voltage and line loading are within the limits. Otherwise, the particle is particle is infeasible.

- Step 3: Compare the objective value of each particle to the best individual value. Set the objective value as the current P_{best} if it is less than P_{best}, and record the corresponding particle position.

- Step 4: Select the particle with the lowest individual best P_{best} of all particles and use the value of this P_{best} to determine the current overall best G_{best}.

- Step 5: Maximum and average fitness levels are computed. The equation; $Error = (maximum fitness minus average fitness)$, is used to calculate the error. Proceed to step 9 if this error is less than a specified tolerance.

- Step 6: Using equations 3.1 and 3.2 respectively, update the particle's velocity and position.

- Step 7: For each particle's new position, new fitness values are calculated. If the new fitness value for any particle is greater than the previous P_{best} value, then the P_{best} value for that particle is set to the current fitness value. Similarly, the G_{best} value is derived from the most recent P_{best} values.

- Step 8: The iteration count is increased, and if the maximum number of iterations is not reached, the process goes back to step 2. Step 9: The optimal DG sizes in and locations are determined by G_{best} particle, and the results are printed.

3.4.3 IEEE 69-bus Test System description

The IEEE 69-bus test feeder is a standard, medium-sized radial distribution system with a total demand of 3,8021 MW and 2,6946 MVAR. Its base voltage is 12.66 kV, and its data is

extracted from [107]. The base power is 100 MVA, and the bus voltage limits shall be set at 0.95 p.u and 1.05 p.u respectively. The overall active and reactive power losses in the standard test system are 224.9304 KW and 102.1321 KVAR. Its network's load and line data are shown in Appendix B.

Figure 3.4 represents the single line diagram of the IEEE 69-bus test system.

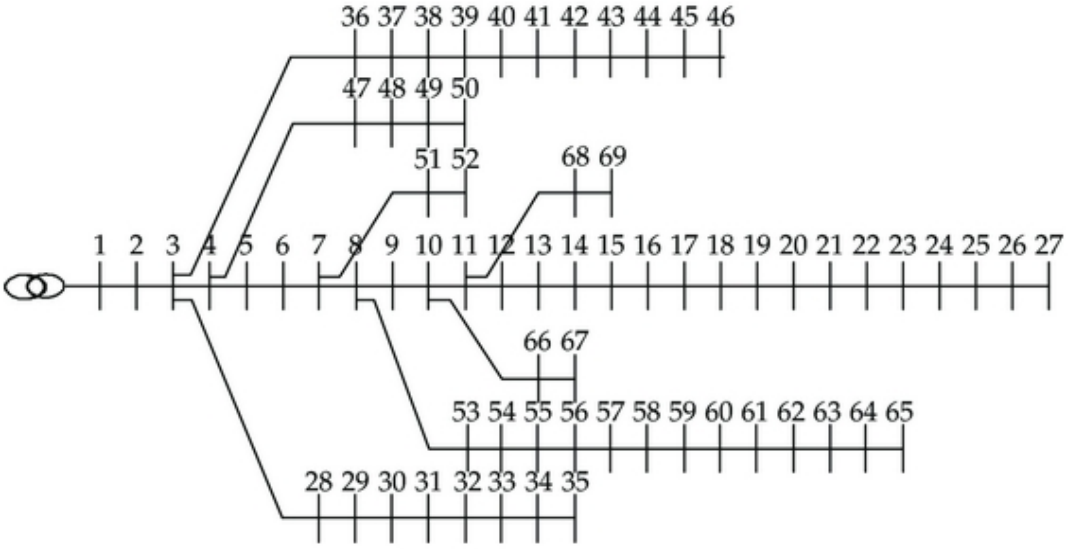

Figure 3.4: IEEE-69 bus Load Single line diagram

Figure 3.5 shows the voltage profile results for the IEEE 69-bus test system after 1781 kW DG penetration at bus 61. The real loss of power has fallen from 224,9304 kW to 83,1997 kW, and the minimum voltage has improved from 0.87 p.u to 0.96 p.u.

3.5 Summary

The existing IEEE-33 bus and IEEE-69 bus test systems are modified in this chapter by adding Distributed Generators (DGs) to them, making them active distribution systems. The DG placement improved the voltage profile and lower the active power loss in the test systems. Particle Swarm Optimization algorithm is used for optimal sizing and placement of the DGs. The Newton-Raphson method was used to calculate the load flow of the modified test systems in MATLAB.

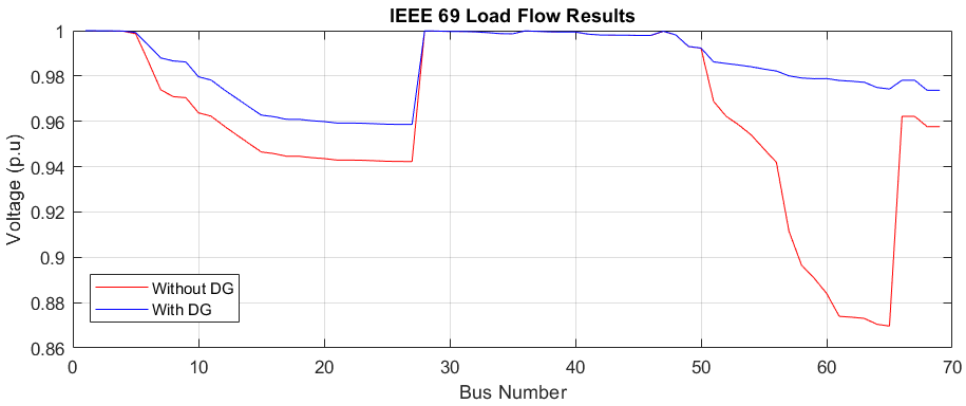

Figure 3.5: IEEE-69 Voltage profile results before and after DG Placement

Chapter 4

State estimation

This chapter presents the measurement data set for state estimation in the modified IEEE-33 bus and IEEE-69 bus test systems and results on the performance of the WLS and EKF state estimation algorithms. The load flow results on the selected test systems are the benchmark of the results. The chapter ends with a comparison of the results of the WLS and EKF state estimation algorithms.

4.1 Measurement data set

The measurement data set used for the load profiles in this dissertation is from the ADRES-CONCEPT project[1]. The project discusses energy use in households including those for heating and electric-motorized transport. The results of analyses of survey data on household electricity and a measurement series for approximately 40 households in upper-Austria were used to develop a model in MATLAB to simulate household load profiles based on different parameters including household size, building type, weekday, seasonality. The measurements at each household was done at an interval of 1 sec, for one week in summer and one week in winter.

The measurement dataset consists of active and reactive power as well as voltage (RMS) values per phase. They are provided as one binary file in MATLAB format (.mat) with the

[1] "ADRES-CONCEPT" (EZ-IF: Development of concepts for ADRES – Autonomous Decentralized Regenerative Energy Systems, project no. 815 674) [108]. This project was funded by the Austrian Climate and Energy Fund and performed under the program "ENERGIE DER ZUKUNFT"

following structure:

- Both matrices (Data.U and Data.PQ) stored in the structure which are of the IEEE data type "single" (32 bits in total, 8 bits for the exponent).

- Data.U is a matrix containing the voltage values (V) per phase and household. The number of rows is 1209600 (2 weeks x 7 days x 24 hours x 3600 seconds). The number of columns is 90 (3 phases x 30 households).

Household 1			...	Household 30		
UL1N	UL2N	UL3N	...	UL1N	UL2N	UL3N

- Data.PQ is a matrix containing the active (P) and reactive power (Var) values per phase and household. The number of rows is 1209600 (2 weeks x 7 days x 24 hours x 3600 seconds). The number of columns is 180 (2 power values x 3 phases x 30 households).

Household 1						...
P_{L1N}	Q_{L2N}	U_{L3N}	U_{L1N}	U_{L2N}	U_{L3N}	...

All measurements were done asynchronously (non-simultaneous measurement in the different households). However, they have been posteriori "synchronised" so that they all start on Monday 00:00:00 (GMT+1) (with correct weekday/non- weekday).

4.2 PMU placement

PMUs were placed on buses 1, 17, 18, 31, 32, 33 (Fig. 4.1) of the IEEE 33-bus test system. Besides bus 1, which is the slack bus, these buses are at the ends of the laterals of the test system with low bus voltage since placement of PMUs at the tail ends will enhance the estimation accuracy for these nodes.

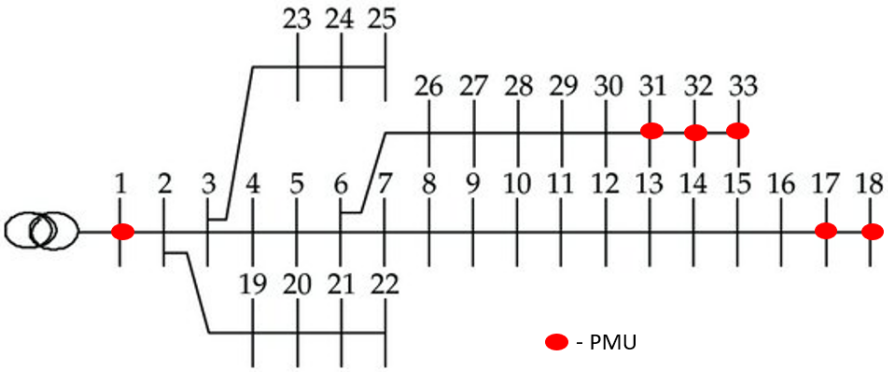

Figure 4.1: PMU placements in the IEEE 33-bus test system

The PMUs were placed on buses 2,3,8,11,14,17,22,26,28,33,34,37,41,45,49,51,56,59,62,64,66, and 68 on the IEEE 69-bus test system. After taking the minimum number of PMUs and the lowest state estimate error as the objective functions and full observability of the distribution network as the constraint, the optimal locations were 22 buses out of a total of 69.

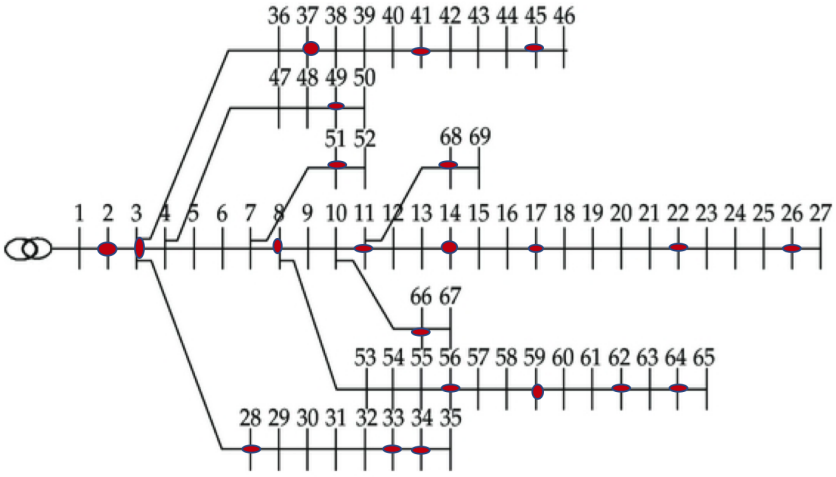

Figure 4.2: PMU placements in the IEEE 69-bus test system

The PSO algorithm (Fig. 4.3) was used to position the PMUs optimally with the goal of increasing observability with the least possible number of PMUs. Similarly, the optimal PMU placement maximises the measurement redundancy, which represents the number of times a bus is observed directly or indirectly [109].

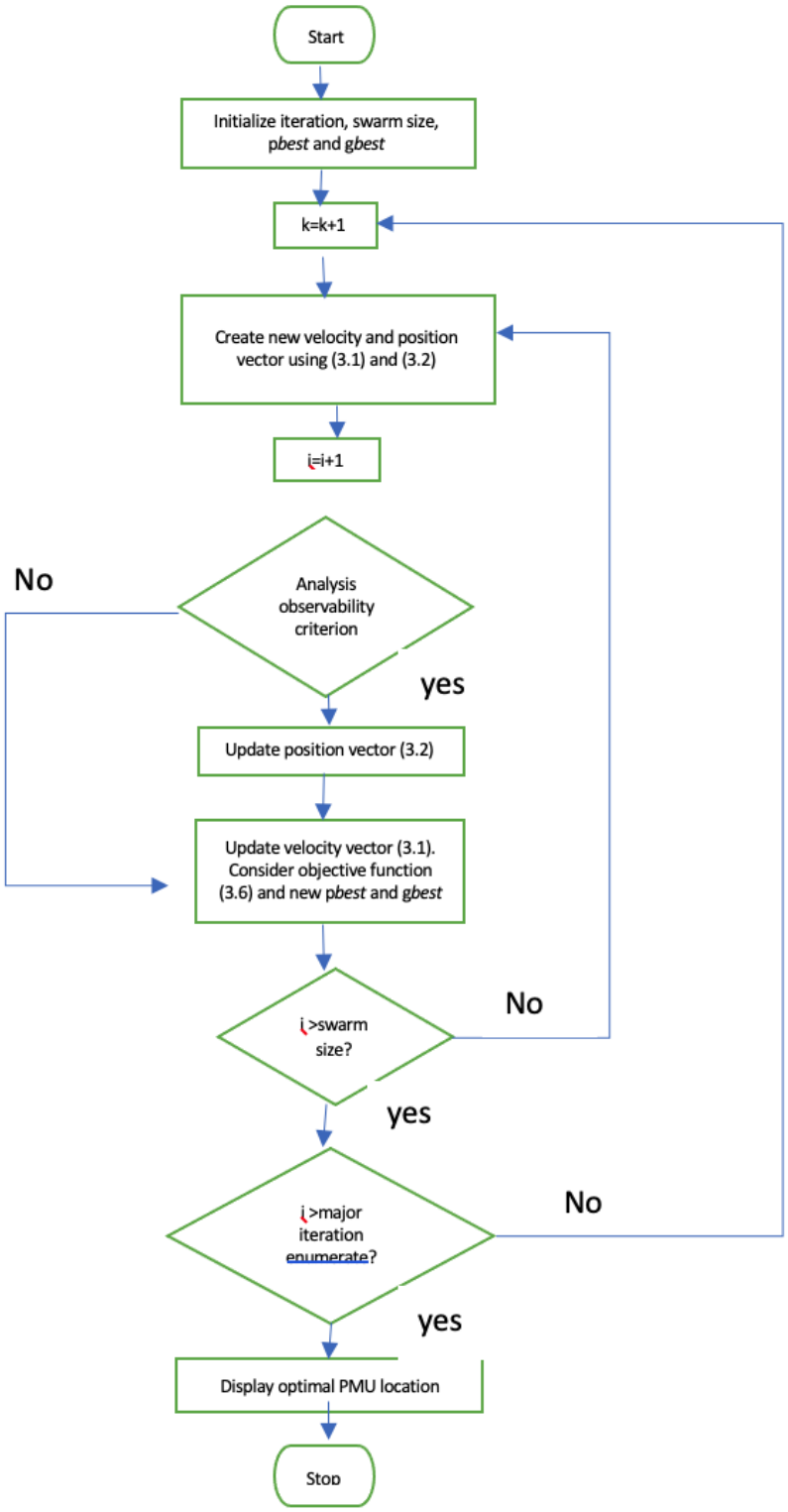

Figure 4.3: PSO flowchart for PMU placement

4.3 WLS formulation for ADSSE

The formulation of the WLS algorithm is based on [110]:

i **The maximum likelihood criterion:** the objective is to maximize the likelihood that the state variable $\hat{x}$ is the correct estimation of the vector x.

ii **The minimum variance criterion:** the objective is to minimise the normal estimation of the sum of squares of the deviations of the estimated components of the state variable.

The conventional WLS SE method determines the state estimate by the minimisation of the squares of the errors of all measurements. For n buses, there would be $(2n-1)$ number of state variables; n voltage magnitudes, and $(n-1)$ voltage angles with one angle taken as reference. Therefore, the number of measurements (m) required to obtain the accurate state estimation should be $m \geq (2n-1)$.

Hence, the network state vector $x \epsilon R^{(2\mathrm{n}\text{-}1)}$ is as follows:

$$x = [\delta_2, ..., \delta_\mathrm{n}, V_1, ...V_\mathrm{n}]^\mathrm{T} \tag{4.1}$$

where δ_i and V_i are the respective phase angle and magnitude of the voltage phasor at bus i

The WLS computes the most likely system state based on distributed measurements (power injections, load flows, line current, voltages) e.g. those from the ADRES-CONCEPT project (section 4.1), pseudo-measurements or load forecasts, and the existing network topology and model. It assumes that all the measurement errors have a known probability distribution and can only be applied to linear models with normal (Gaussian) distributed noise, whose mean, μ and the variance, σ^2 are assumed to be known [111].

The normal probability density function (p.d.f) of measurement z_i is defined as:

$$f(z_\mathrm{i}) = \frac{1}{\sqrt{2\pi}\sigma_\mathrm{i}} e^{(-\frac{1}{2}(\frac{z_\mathrm{i}-\mu_\mathrm{i}}{\sigma_\mathrm{i}})^2} N(\mu_\mathrm{i}, \sigma_i^2) \tag{4.2}$$

And the joint p.d.f $f_m(z)$ is the product of the individual p.d.fs. It expresses the likelihood of

observing a specific measurement set in the measurement array z^T.

$$f_{\mathrm{m}}(z) = f(z_1)f(z_2)...f(z_{\mathrm{m}}) \tag{4.3}$$

Where z $_{\mathrm{i}}$ is the i $^{\mathrm{th}}$ measurement, m is the total number of measurements and:

$$z^{\mathrm{T}} = [z_1, z_2...., z_{\mathrm{m}}] \tag{4.4}$$

After linking $f_{\mathrm{m}}(z)$ with the power system state, the objective of the WLS is to maximize $f_{\mathrm{m}}(z)$ by varying the unknown system state. This is expressed as:

$$\begin{aligned} &\text{Maximise} \quad \log f_{\mathrm{m}}(z) \\ OR& \\ &\text{Minimise} \quad \sum_{i=1}^{m} (\frac{z_{\mathrm{i}} - \mu_{\mathrm{i}}}{\sigma_{\mathrm{i}}})^2 \end{aligned} \tag{4.5}$$

Equation 4.5 does not contain the system state explicitly. It is formulated as a function of the i$^{\mathrm{th}}$ measurement's residual r$_{\mathrm{i}}$ in order to express its link to the system's state.

$$r_{\mathrm{i}} = z_{\mathrm{i}} - \mu_{\mathrm{i}} \tag{4.6}$$

where μ_{i} is expressed as a function of the system state x i.e. $h_{\mathrm{i}}(x)$, which is the measurement function relating the system state to the i$^{\mathrm{th}}$ measurement. The square of each residual r_i^2 is weighted by $W_{ii} = \sigma_i^{-2}$, hence (4.5) above can be rewritten as:

$$\begin{aligned} &\text{Minimise} \quad \sum_{i=1}^{m} W_{ii} r_i^2 \\ &\text{Subject to} \quad z_{\mathrm{i}} = h_{\mathrm{i}}(x) + r_i, \quad \text{for} \quad i = 1, ..., m \end{aligned} \tag{4.7}$$

The WLS estimator must minimise the objective function (4.8) in order to resolve (4.7) and obtain the state estimate result.

$$J(x) = \sum_{i=1}^{m} \frac{(Z_i - h_i(x))^2}{R_{ii}} \tag{4.8}$$

where $R_{ii} = diag(\sigma_1^2, \sigma_2^2, \ldots, \sigma_m^2)$ is the measurement noise covariance matrix.

In matrix form, the objective function is rewritten as:

$$\text{Minimise} \quad J = [z - h(x)]^{\mathrm{T}} R^{-1} [z - h(x)] \tag{4.9}$$

Since $h(x)$ is non-linear, it is tough to minimise. Thus, measurement function is differentiated with respect to the state variables to satisfy the optimal first-order conditions; expressed as follows:

$$g(\hat{x}_t) = \left. \frac{\partial J(X_t)}{\partial X_t} \right|_t = H^T (\hat{X}_t R_t^{-1} [z_t - h(\hat{x}_t)]) = 0 \tag{4.10}$$

The measurement function $h(x_t)$ can be linearized around a generic vector ($\hat{x}_{t,k}$) yielding;

$$H^T(\hat{x}_{t,k}) R_t^{-1} [z_t - h(\hat{x}_t)] - G(\hat{X}_{t,k})(\hat{x}_{t,k+1} - \hat{x}_{t,k}) = 0 \tag{4.11}$$

Where G is the Gain matrix and k is the iteration index. Therefore:

$$\hat{x}_t^{k+1} = \hat{x}_t^k + [G(\hat{x}_t^k)] H^T(\hat{x}_{t,k}) R_t^{-1} [z_t - h(\hat{x}_t)] \tag{4.12}$$

where: $G(\hat{x}_t^k) = \frac{\partial g(\hat{x}_t)}{\partial x_t]^k}$

The calculation and triangular decomposition of the Gain matrix is the key computational burden associated with the WLS state estimation. One way of reducing this burden is to keep the Gain matrix constant. The DSSE problem may not converge if the gain matrix is ill-conditioned [2].

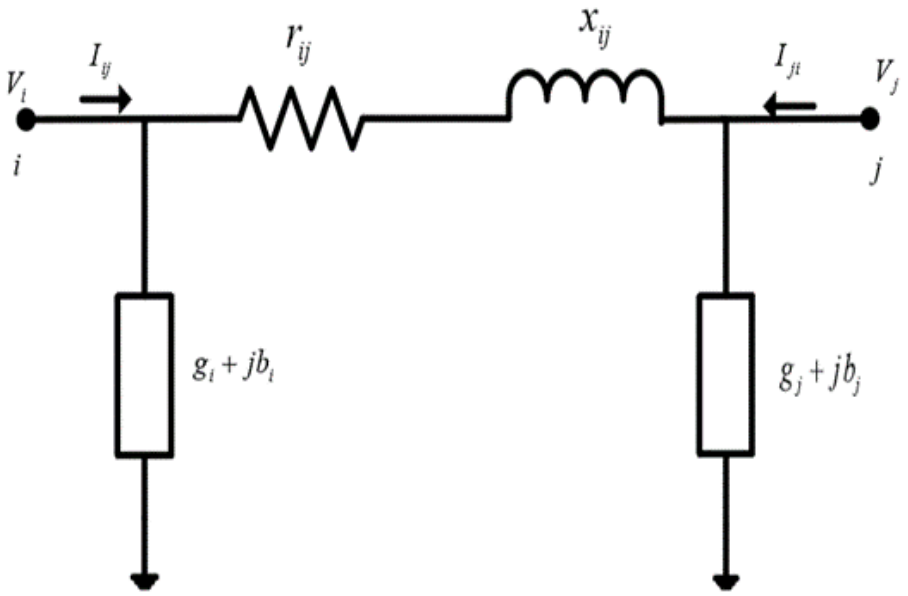

Figure 4.4: Two-port transmission line $\pi - model$

4.3.1 Measurement function

The two-port transmission line π-model in Fig. 4.4 is used to relate the state vector variables to each type of the measurements. The usual choice for state variables is the bus voltage phase angles and magnitudes, while the measurements are active and reactive power flows, node injections and voltage magnitudes. With the assumption that all the parameters of the system, such as the impedance of the branches, tap positions of the transformer and the state of the circuit breakers, and at least two of the four variables are known, the remaining variables can be calculated using $z = h(x) + r$. The most typical iterative method of solving the equation is the Newton-Raphson method, where the measurement function $h(x)$ can map the state of the system to its bus voltage magnitudes, bus power injection, and the power flow measured in the network.

Line Power Flows

Considering the two-port -model, the expressions of the line power flows P_{ij} and Q_{ij} are given by:

$$P_{ij} = V_i^2(g_{ij} + g_p^{sh}) - V_iV_j(g_{ij}\cos\delta_{ij} + b_{ij}\sin\delta_{ij}) \tag{4.13}$$

$$Q_{ij} = -V_i^2(b_{ij} + b_p^{sh}) - V_iV_j(g_{ij}\sin\delta_{ij} - b_{ij}\cos\delta_{ij}) \tag{4.14}$$

where V_i and δ_i are the bus voltage magnitudes and phase angles at the i^{th} bus, $g_{ij} + jb_{ij}$ is the series admittance between buses i and j, $g_p^{sh} + jb_i^{sh]}$ is the shunt admittance at the i^{th} bus, and $\delta_{ij} = \delta_i - \delta_j$.

Bus power injections

The bus power injections at the i^{th} bus is expressed as:

$$P_i = V_i \sum_{j=0}^{N} V_j (G_{ij} \cos\theta_{ij} + B_{ij} \sin\theta_{ij}) \tag{4.15}$$

Where N is the number of buses connected to the i^{th} bus and $G_{ij} + jB_{ij}$ is the ij^{th} element 0f the bus admittance matrix [112].

Line currents

The line currents in the ij^{th} is:

$$I_{ij} = \frac{\sqrt{P_{ij}^2 + Q_{ij}^2}}{V_i} \tag{4.16}$$

Measurement Jacobian

From the measurements above, the jacobian matrix of the measurements is:

$$H = \frac{\partial h(x)}{\partial x} \tag{4.17}$$

It consists of the partial derivatives of equality constraints with respect to the state variables

The WLS algorithm as implemented in this study is summarized below and depicted in Fig. 4.5.

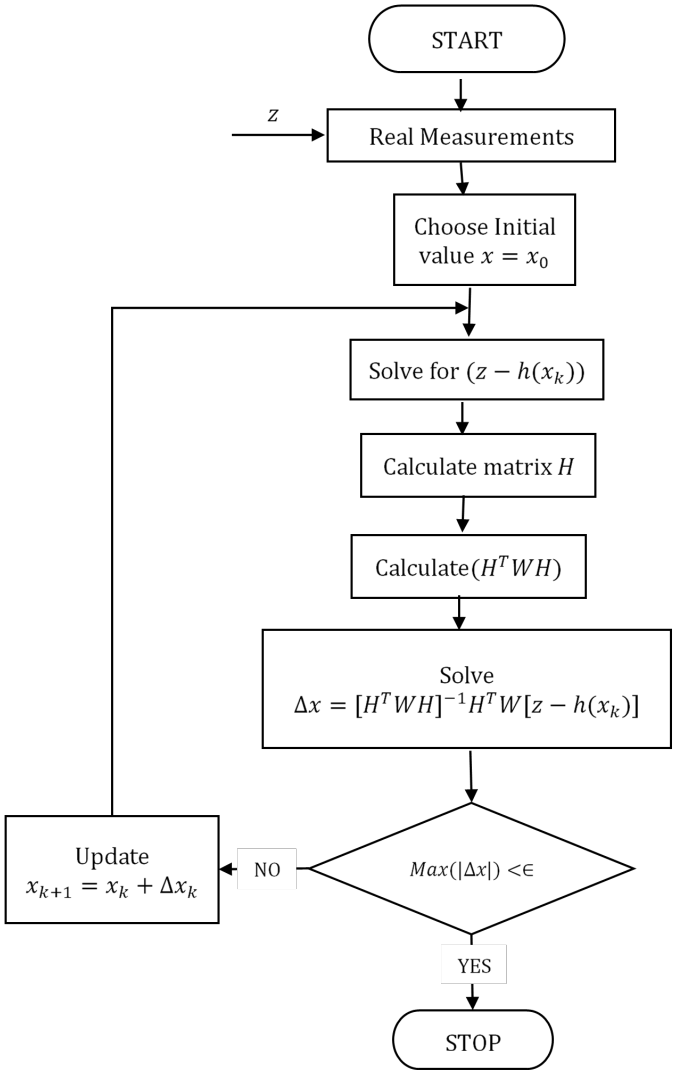

Figure 4.5: WLS flow chart

Summary of WLS iterative process

WLS iterative algorithm process

1: Initialize the state vector x^0, starting as a flat-rate with all bus voltages at 1 p.u and the angles are zero
2: Calculate the nonlinear measurement function $h(x^k)$ and the jacobian matrix $H(\hat{x}_t^k)$
3: Compute the gain matrix $G(\hat{x}_t^k)$ and the function $g(\hat{x}_t)$
4: $\hat{x}_t^{k+1} = \hat{x}_t^k + [G(\hat{x}_t^k)]H^T(\hat{x}_{t,k})R_t^{-1}[z_t - h(\hat{x}_t)]$
Stopping criteria
5: Calculate $J(\hat{x}_t^k)$ and stop if the following conditions are met:
- $\max |\hat{x}_t^{K+1} - \hat{x}_t^K| \leq \epsilon_1$
- $|J\hat{x}_t^{K+1} - J\hat{x}_t^K| \leq \epsilon_2$
- $J\hat{x}_t^{K+1} < \epsilon_3$

where: $\epsilon_{1,2,3}$ are pre-selected thresholds in the order of 0.0004

4.3.2 WLS Results

The following assumptions were used in implementing the WLS SE algorithm:

- The measurement noises are Gaussian-distributed with an average mean of zero.
- The measurement noises are uncorrelated; therefore they are weighted according to their accuracy. Hence, the measurement noise matrix R is diagonal, which minimizes the total weighted value of squared residuals in the WLS process.
- The network is observable

The voltage magnitude profile calculated with WLS is compared with that from the load flow results in Fig. 4.6 The WLS-estimated voltage profile closely resembles that from standard load flow using the Newton-Raphson algorithm. The estimation error calculated using $|V_{true} - V_{WLS}|$ are within the allowable error range (Fig. 4.7). The highest deviations of the estimations from the true values are observed at the nodes that are at the ends of the laterals of the test system. This justifies the placement of the PMUs at these nodes to improve the accuracy of the state estimation (Fig. 4.1). The maximum error of 0.0068 occurs at bus 32.

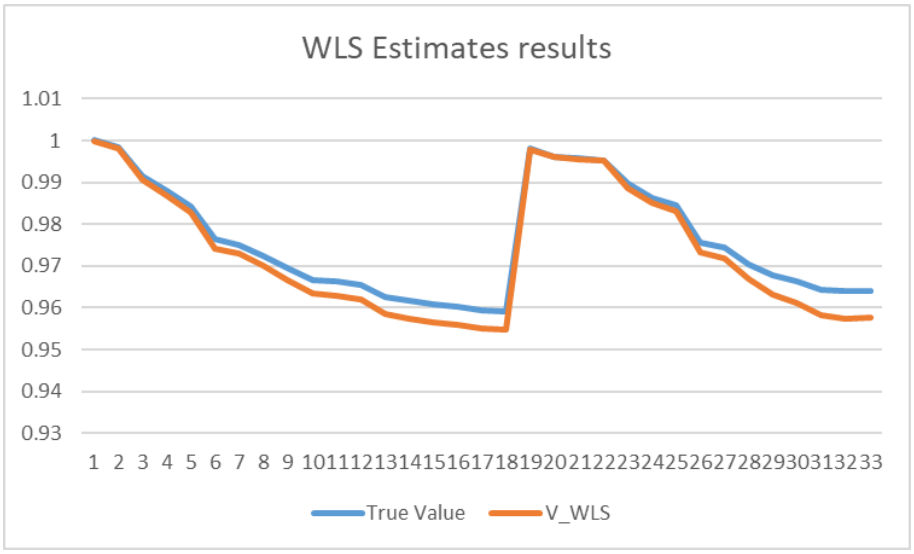

Figure 4.6: Comparison of the IEEE 33-bus test system voltage magnitude profile estimated using WLS with that from load flow analysis (true value)

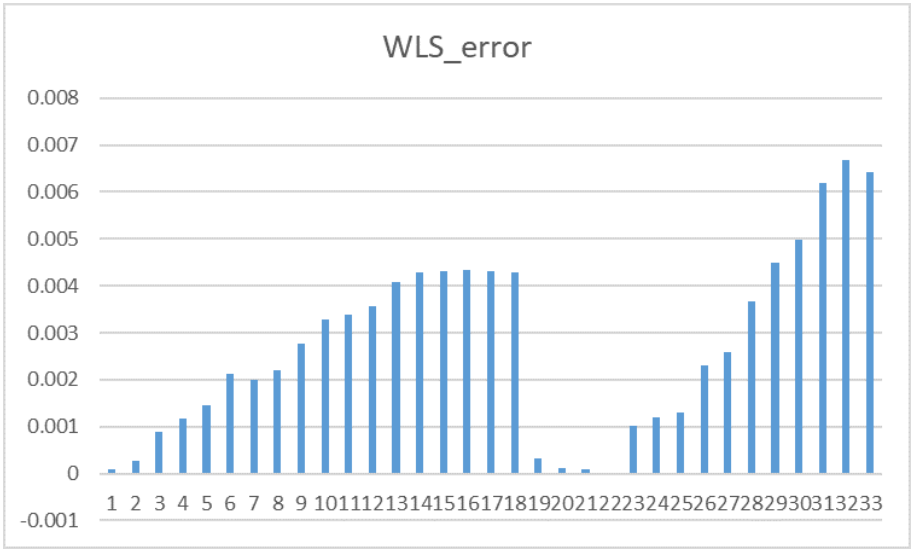

Figure 4.7: Error in WLS estimates of IEEE 33-bus test system voltage magnitude profile

The voltage phase angle estimation results are shown in Fig. 4.8. The estimation errors are slightly greater than those for voltage magnitude, but they are still within the allowable error range.

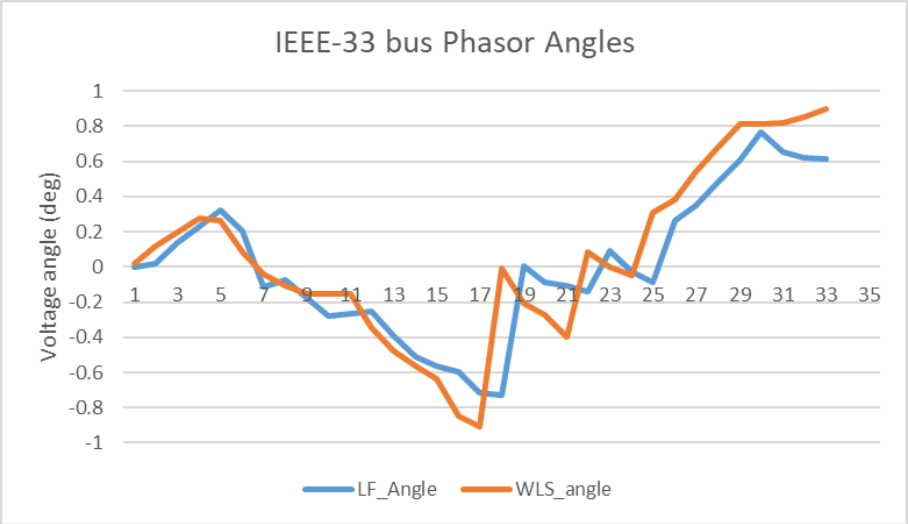

Figure 4.8: Comparison of IEEE 33-bus test system voltage phase angle profile estimated using WLS with that from load flow analysis (true value).

4.4 EKF formulation for ADSSE

The EKF is made up of two parts, the a priori (prediction/process), based on the prior state estimate computed in the previous iteration, this estimate is computed before any system measurements are made, and a posteriori (measurement-update/estimation). The EKF is based on these assumptions:

- The measurement and process noise are Gaussian and uncorrelated.
- The network is observable.

The basic mathematical formulation of the EKF is given by (4.18) and (4.19):

$$x_k = g(u_k, x_{k-1}) + \epsilon_k \tag{4.18}$$

$$z_k = h(x_k) + \delta_k \tag{4.19}$$

where ϵ_k is the process noise and δ_k is the measurement noise, with zero mean. The functions g and h must be linearized by computing their Jacobian matrices.

At every time step (k), the EKF algorithm represents the estimation x_k by its mean μ_k and

covariance Cov_k. The calculation of the mean and the covariance occurs in two steps:

1. Prediction

$$\bar{\mu}_k = g(u_k, \mu_{k-1}) \tag{4.20}$$

$$Cov_k = G(u_k, \mu_{k-1}) \sum_{k-1} G^T(u_k, \mu_{k-1}) + Q \tag{4.21}$$

2. Correction

$$K_k = \bar{\sum}_k H^T(\bar{\mu}_k)[H(\bar{\mu}_k) \bar{\sum}_k H^T(\bar{\mu}_k) + R]^{-1} \tag{4.22}$$

$$\mu_k = \bar{\mu}_k + K_k[z_k - h(\bar{\mu}_k)] \tag{4.23}$$

$$Cov_k = [I - K_k H(\bar{\mu}_k)]\overline{Cov_k} \tag{4.24}$$

where $g(u_k, \mu_{k-1})$ is linearized around the mean μ_{k-1}, $G(u_k, \mu_{k-1}) = \frac{(u_k, \mu_{k-1})}{\partial x_{k-1}}|_{x_{k-1}=\mu_{k-1}}$ and Q is the covariance of the noise matrix. The matrices H, h and R are the same as in the WLS method.The measurement z_k is only incorporated in the algorithm during the correction step. K_k is the kalman gain, and it specifies to which degree the measurements are incorporated into the new state estimate. Consequently, every iteration uses a new set of measurement for the correction step. Nonetheless, it can be assumed that the mean remains constant since the state of the power system hardly changes during the consecutive time steps. Therefore, (4.20) becomes:

$$\bar{\mu}_k = \mu_{k-1} \tag{4.25}$$

Thus, it follows that g is independent of u_k and $G(u_k, \mu_{k-1}) = \frac{(u_k, \mu_{k-1})}{\partial x_{k-1}}|_{x_{k-1}=\mu_{k-1}}$ becomes an identity matrix. The updated EKF formulation is:

1. Prediction

$$\bar{x}_k = x_{k-1} \tag{4.26}$$

$$\bar{\sum}_k = \sum_{k-1} + Q \tag{4.27}$$

2. Correction

$$K_k = \bar{\sum}_k H^T(\bar{x}_k)[H(\bar{x}_k) \bar{\sum}_k H^T(\bar{x}_k) + R]^{-1} \tag{4.28}$$

$$x_k = \bar{x}_k + K_k[z_k - h(\bar{x}_k)] \tag{4.29}$$

$$\sum_k = [I - K_k H(\bar{x}_k)] \bar{\sum}_k \tag{4.30}$$

The EKF can be used instead of the WLS approach where there is a prior understanding of the states. This foreknowledge is represented by the covariance matrix Q.

The steps for implementing the EKF are summarized below. It is assumed that at any time instant initial estimates, x_0 are known and its corresponding covariance matrix, P_k^0 is also known.

EKF algorithm

1: initialise initial estimate and its associated covariance matrix
2: read the measurement inputs data sets
3: calculate Δz_k
4: calculate Jacobian matrix H_k
5: calculate Kalman gain $G_k = P_0 H_k^T (H_k P_K^0 H_k^T + R)^{-1}$
6: Solve for $\Delta_x = G_k(\Delta Z_k - h(x_k))$
7: update error covariance matrix,

$$P_k = (I - G_k H_k) P_k^0$$

$$P_{k+1}^0 = P_k + Q_k$$

Stopping criteria

8: above steps are repeated for allowable tolerance limit of Δ_x

4.5 EKF results

The test system voltage magnitude profile obtained using the EKF closely resembles that from load flow analysis, which was used for benchmarking (Fig. 4.9). The deviations are within acceptable limits, with the maximum deviation of 0.006 at bus 33 (Fig. 4.10)

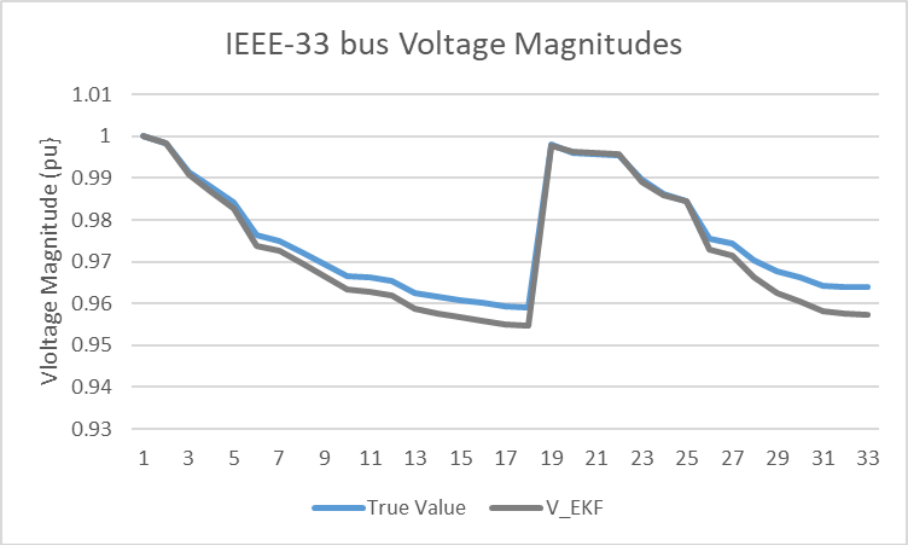

Figure 4.9: Comparison of IEEE 33-bus test system voltage phase angle profile estimated using EKF with that from load flow analysis (true value).

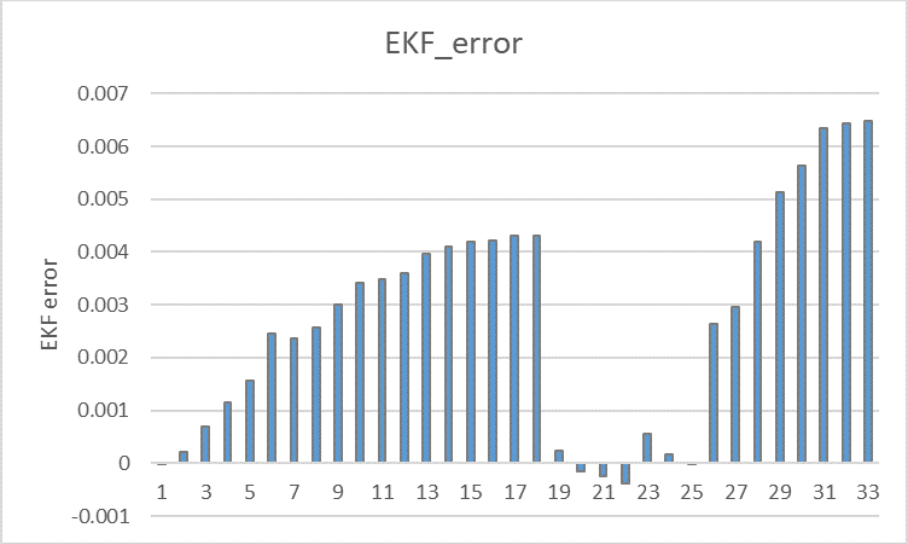

Figure 4.10: EKF results' deviation from the True Value

The EKF method is equally capable of approximating the voltage phasor angles on the selected bus test system with enough accuracy (Fig. 4.11).

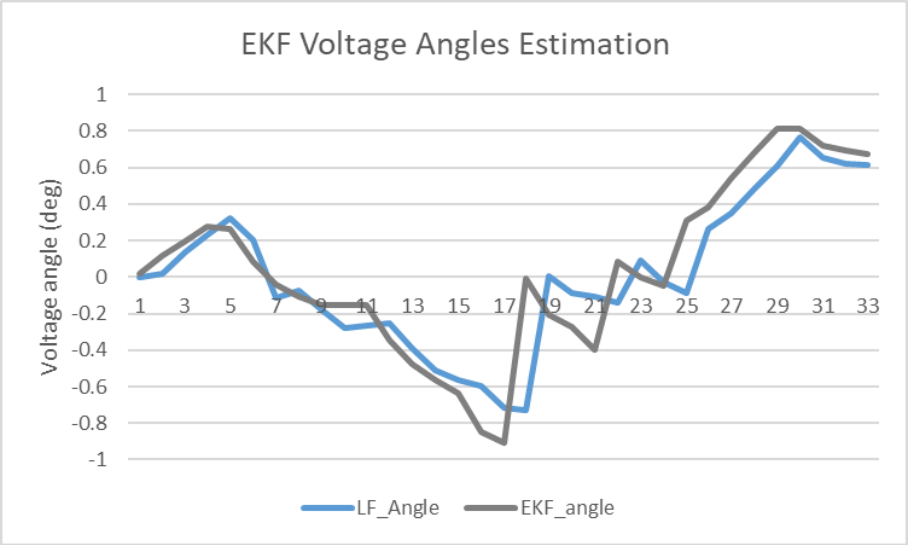

Figure 4.11: Comparison of IEEE 33-bus test system voltage phase angle profile estimated using EKF with that from load flow analysis (true value).

4.6 Comparison of WLS and EKF results

This section compares the performance of the results obtained using the WLS and EKF algorithms respectively. The load flow results are used as the benchmark. A comparison of voltage magnitude estimations by each algorithm against the benchmark are shown in Fig. 4.12. Fig. 4.12 compares the deviations of the voltage magnitude estimations by the WLS and EKF from the true value.

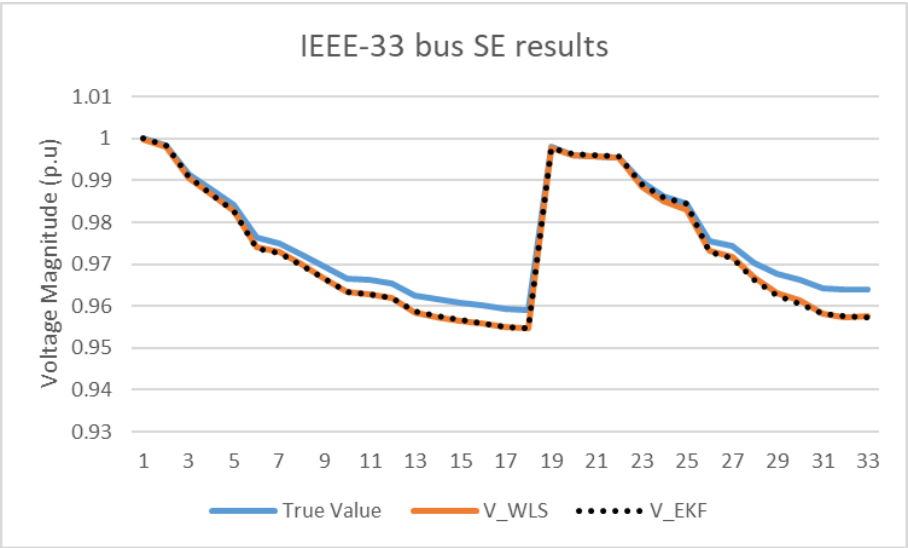

Figure 4.12: IEEE 33-bus test feeder voltage profiles obtained from load flow, WLS and EKF

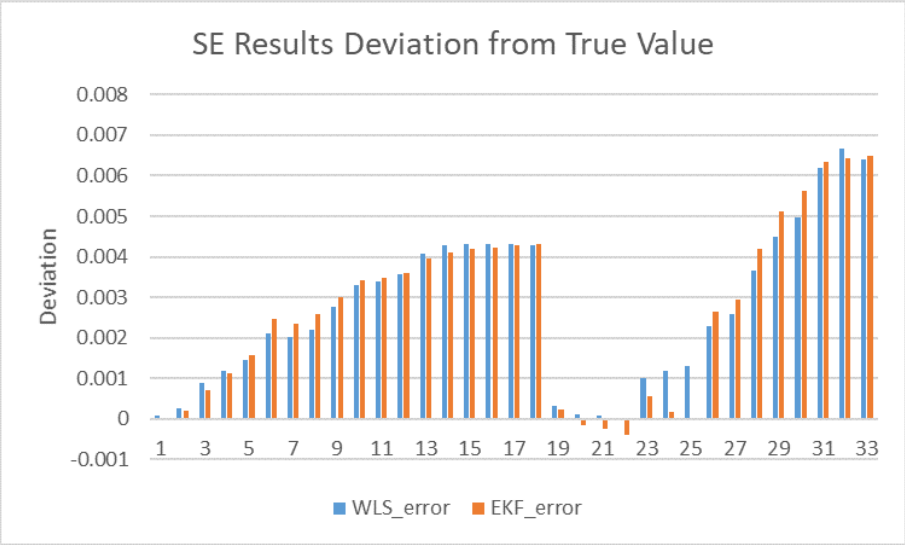

Figure 4.13: Deviations of the voltage magnitude estimations by the WLS and EKF from the true value.

The root mean squared error (RMSE) (4.31), which is the square root of the mean of the square of all the deviations from the true value (load flow results) and the correlation equation 4.32, are used as the metric for comparing both algorithms. The RMSE provides information about a model's short-term performance by allowing for a term-by-term comparison of the actual difference between the estimated and measured values. The lower the value, the better the performance of the model.

$$RMSE = \sqrt{\frac{1}{n}\sum_{i=1}^{n}(V_{true} - V_{estimate})^2} \tag{4.31}$$

where $V_{estimate}$ are the SE results, V_{true} is the true value (load flow results), and n is the total number of buses. The average RMSE is 0.00025168 and 0.00020588 for the WLS and EKF respectively.

Numerical analysis of the RMSE values shows that the EKF is slightly more accurate than WLS. However, it should be noted the EKF makes use of the past and present measurements, whereas the WLS only uses measurements from the current time-step. Hence, the EKF should intuitively perform better. Paolone et al. [113] proved that the state estimation error with the recursive algorithm is always less than the estimation error from the WLS method. The estimation difference is equal to the mean of the squared difference between the two

methods as shown in (4.32) and illustrated by Fig. 4.14 from the numerical validation of this result.

$$\mathbf{E}[|x_t - \bar{x}_{t,WLS}|^2] = \mathbf{E}[|x_t - \bar{x}_{t,EKF}|^2] + \mathbf{E}[|\bar{x}_{t,WLS} - \bar{x}_{t,EKF}|^2] \tag{4.32}$$

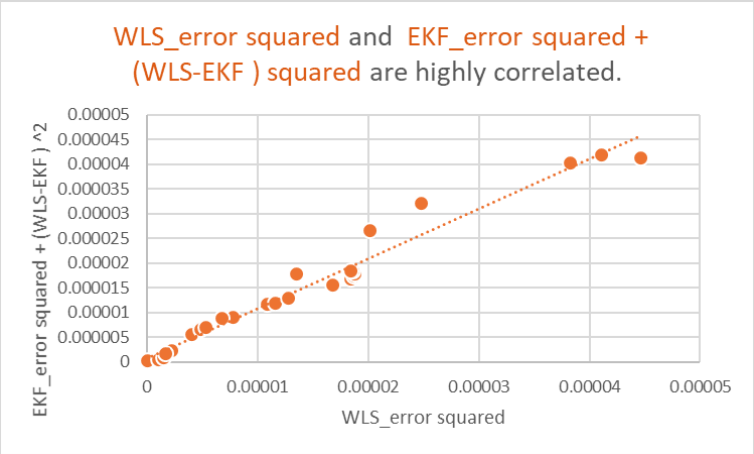

Figure 4.14: Correlation between WLS_{error} squared and EKF_{error} squared plus mean square difference between WLS and EKF results

4.7 ADSSE on modified IEEE 69-bus

The state estimation was also performed on the IEEE 69-bus to show the scalability of this research and compared using the same metrics as in the IEEE 33-bus experiments.

Figure 4.16 shows the voltage magnitudes obtained from the load flow, WLS and EKF methods, while Figure 4.15 shows the respective phasor angles.

The average RMSE is 0.006239776 and 0.010576188 for the WLS and EKF respectively.

4.8 Performance of WLS and EKF on standard IEEE 33-bus and IEEE 69-bus

Figure 4.17 shows the voltage magnitude results from both the WLS and EKF algorithm on a standard IEEE 33-bus. A standard IEEE 33-bus is one where no DG is placed. This section compares the performance of the two algorithms when there is no DGs in the system.

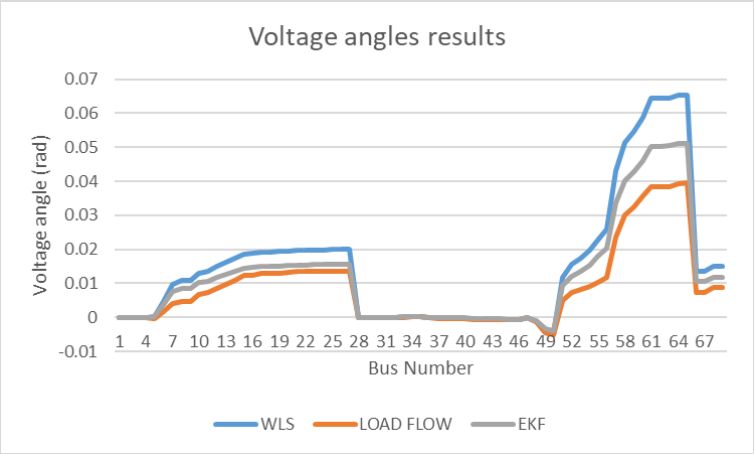

Figure 4.15: IEEE 69-bus test feeder voltage angles obtained from load flow, WLS and EKF

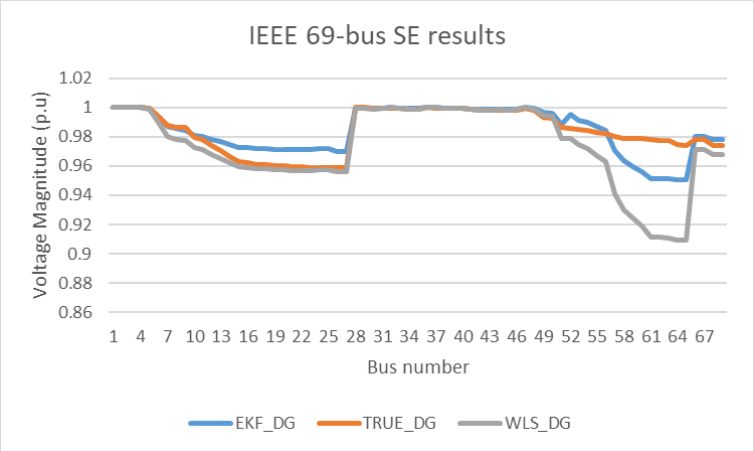

Figure 4.16: IEEE 69-bus test feeder voltage profiles obtained from load flow, WLS and EKF

Both algorithms produce precise results that are strongly correlated, but EKF is still the nearest to the expected results.

The EKF algorithm performs better because it not only estimates the current system's state but also predicts the state at the next sampling time. Static methods such as the WLS do not have a foreknowledge of the system. Therefore, the EKF still shows more accurate results under less time and after fewer iterations in a standard distribution system as in active distribution systems.

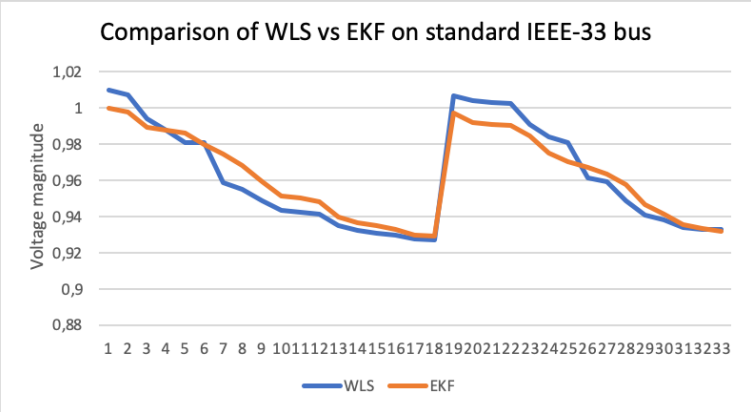

Figure 4.17: WLS and EKF Voltage magnitude estimation results on a standard IEEE 33-bus

Similarly, the same results are observed in the IEEE 69-bus as seen in Fig. 4.18

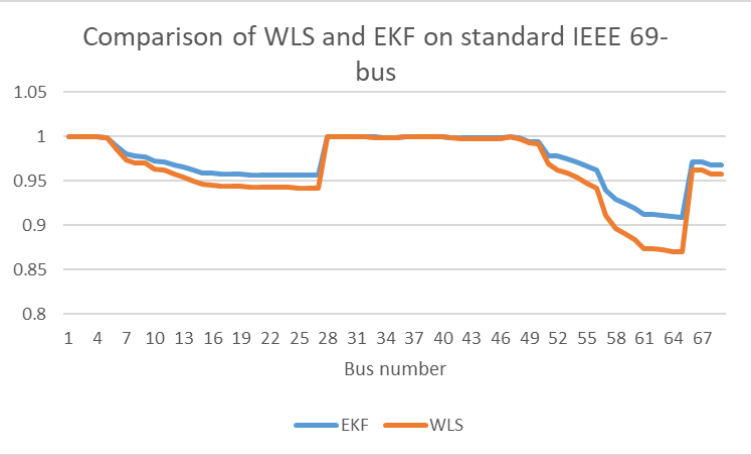

Figure 4.18: WLS and EKF Voltage magnitude estimation results on a standard IEEE 69-bus

4.9 Summary

This chapter compares the performance of the WLS and EKF algorithms in terms of accuracy and computing time, as well as the placement of PMUs in modified IEEE-33 and IEEE-69 test bus systems using the PSO method. The following assumptions are used in this analysis: (1) There are no systematic errors; (2) the linear measurement model is known; (3)high time-resolution measurements from PMUs is used; and (4) there are no bad-data and network model errors.

The WLS computes the most likely system state based on distributed measurements (power injections, load flows, line current, voltages) from the ADRES-CONCEPT project, pseudo-measurements or load forecasts, and the existing network topology and model. The EKF is a two-step state estimation algorithm which is best suited for non-linear systems whose prior state estimate is known. The case studies consist in the IEEE-33 bus system and the IEEE-69 bus test feeder that are modified to include Distributed Generation. The theory predicts that EKF is more accurate than the WLS if the process model is correct. The experiments carried out in this dissertation statistically validated that EKF is indeed a better performer in state estimation than WLS because it not only estimates the current system's state but also predicts the state at the next sampling time. The EKF shows more accurate results under less time and fewer iterations.

Chapter 5

Conclusion

The research undertaken for this dissertation was motivated by the current trends in the inclusion of DGs closer to the consumer, which necessitates the need for real-time visibility throughout the distribution network. Active distribution state estimation is paramount now more than ever, especially in attaining smart grid goals of DG inclusion, demand-responsive loads and smart metering. Thus, the development of ADSSE is inevitable for the implementation of protection, optimisation, control techniques and other smart grid technologies.

As discussed in section 2.4, the main challenge in ADSSE is the limited number of real-time measurements. This research addresses this issue by placing six PMUs on the IEEE 33-bus test system, which was modified to include a DG unit. The PSO algorithm was used for both optimal DG and PMU placement. The PMUs were placed on the slack bus and the tail-end buses of the test system (i.e. buses 1, 17, 18, 31, 32, 33) where they effectively enhance the system's observability. The estimation errors for these buses are normally larger than the others because of their high electrical distance from the slack bus (bus 1). The load data of the test system were used as the base case for nodal power injections for the SE process.

The objective of this dissertation is to investigate the performance of the WLS and EKF state estimation algorithms on active distribution systems. The algorithms' performances are evaluated on modified IEEE 33-bus and IEEE-69 bus test systems, with conventional load ow results serving as benchmarks. The PSO algorithm is used to optimize the integration of DG units and PMUs in the test system. Real-world data from the ADRESCONCEPT

project is used to simulate real-world energy consumption.

The performance of WLS and EKF SE active distribution network algorithms were compared based on their accuracy and computation times.

The load flow results were used as the reference case for the SE. The results in section 4.6 show that EKF has a smaller RMSE, which demonstrates that the EKF results are closer to the load flow results (true value). However, EKF has a higher average computational time (68 ms) than WLS (59 ms). Therefore, there is a trade-off between accuracy and the need for higher computational power and speed. In addition, the EKF method showed better performance in network topology identification. It solved the SE problem after three iterations, while the WLS converged on the fourth iteration. It is noteworthy to state that although both techniques perform almost similarly, EKF has an edge over WLS due its foreknowledge about the state. It is therefore recommended as a more robust and reliable estimator suitable for the scenario of unpredictable active distribution networks.

Further, the results shows that apart from having correct input data, having a robust state estimator is important in implementing ADSSE. State estimation is only as accurate as its measurement information, interpreted up-to-date network topology and modern communication infrastructure to support real-time measurement updates. The outputs of ADSSE are instrumental in power system control and protection. Therefore, it is important that utilities employ accurate SE procedures. However, this research shows that the main challenges in ADSSE adoption is not in the formulation of the algorithms but in the input data by showing that the use of the pseudo-measurements together with real time data from PMUs and smart meters improves the state estimation results.

SE is well established in transmission systems than in distribution systems primarily because transmission networks are monitored redundantly. On the other hand, distribution networks have been passive until recently. In essence, the transmission system' SE algorithms are very similar in formulation with the distribution systems'. The main difference is the amount (redundancy) and quality of the measurement and network topology data fed into them. The capabilities of ADSSE are limited in bad data detection and network model correction, which can essentially be addressed by state-of-the-art measuring infrastructure like PMUs. Bad data detection and correction is only effective where there is measurement redundancy. Pseudo-measurements and load forecasts are used in ADSSE to create the threshold levels of observability needed. However, the pseudo-measurements cannot be considered during the

bad data detection process since even the most accurate pseudo-measurements are likely to be less accurate than real-time measurements. Therefore, utilities should invest in upgrades of measurement infrastructure to make positive strides in ADSSE.

As much as this research proves the robustness of WLS and EKF in active distribution systems, it is only based on a synthetic ideal IEEE test grids, and it does not address some major ADSSE challenges. Some of the implementation challenges that need to be addressed on actual grid state estimation include:

- Observability: most practical ADSSE implementation rely on load forecasts as pseudo-measurement to ensure observability. Therefore, the stochastic nature of DGs must be factored in future research. Modern technology like machine learning on smart meter data can be leveraged for load forecasting in real-time DSSE.

- Communication infrastructure: application of PMUs in DSSE is important. Further research should focus on advancement and challenges in telecommunication of PMU data to phasor data collectors.

- Complexity of network: active distribution networks' topologies are always changing, and this must be reflected in dynamic real-time DSSE. AMI is a powerful tool for obtaining this information, but with the high cost of placing the measurement infrastructure on the distribution network, it is necessary to optimize the measurement upgrades at their locations and number.

References

[1] F. C. Schweppe and J. Wildes, "Power system static-state estimation, part i: Exact model," *IEEE Transactions on Power Apparatus and systems*, no. 1, pp. 120–125, 1970.

[2] A. Abur and A. G. Exposito, *Power system state estimation: theory and implementation*. CRC press, 2004.

[3] A. Monticelli, *State estimation in electric power systems: a generalized approach*. Springer Science & Business Media, 2012.

[4] A. E. Kahunzire and K. O. Awodele, "Improving distribution network state estimation by means of phasor measurement units," in *2014 49th International Universities Power Engineering Conference (UPEC)*. IEEE, 2014, pp. 1–6.

[5] H. Liao and J. V. Milanovic, "Pathway to cost-efficient state estimation of future distribution networks," in *2016 IEEE Power and Energy Society General Meeting (PESGM)*. IEEE, 2016, pp. 1–5.

[6] A. L. Da Silva, S. P. Ribeiro, V. Arienti, R. Allan, and M. Do Coutto Filho, "Probabilistic load flow techniques applied to power system expansion planning," *IEEE Transactions on Power Systems*, vol. 5, no. 4, pp. 1047–1053, 1990.

[7] N. Nusrat, "Development of novel electrical power distribution system state estimation and meter placement algorithms suitable for parallel processing," Ph.D. dissertation, Brunel University London, 2015.

[8] F. Ahmad, A. Rasool, E. Ozsoy, R. Sekar, A. Sabanovic, and M. Elita, "Distribution

system state estimation-a step towards smart grid," *Renewable and Sustainable Energy Reviews*, vol. 81, pp. 2659–2671, 2018.

[9] H. Iwata and K. Okada, "Greenhouse gas emissions and the role of the kyoto protocol," *Environmental Economics and Policy Studies*, vol. 16, no. 4, pp. 325–342, 2014.

[10] T. S. Basso and R. DeBlasio, "Ieee 1547 series of standards: interconnection issues," *IEEE Transactions on Power Electronics*, vol. 19, no. 5, pp. 1159–1162, 2004.

[11] J. Watitwa and K. Awodele, "A review on active distribution system state estimation," in *2019 Southern African Universities Power Engineering Conference/Robotics and Mechatronics/Pattern Recognition Association of South Africa (SAUPEC/RobMech/PRASA)*. IEEE, 2019, pp. 726–731.

[12] F. Shabani, M. Seyedyazdi, M. Vaziri, M. Zarghami, and S. Vadhva, "State estimation of a distribution system using wls and ekf techniques," in *2015 IEEE International Conference on Information Reuse and Integration*. IEEE, 2015, pp. 609–613.

[13] M. Todescato, R. Carli, L. Schenato, and G. Barchi, "Smart grid state estimation with pmus time synchronization errors," *Energies*, vol. 13, no. 19, p. 5148, 2020.

[14] D. Macii, D. Fontanelli, and G. Barchi, "A distribution system state estimator based on an extended kalman filter enhanced with a prior evaluation of power injections at unmonitored buses," *Energies*, vol. 13, no. 22, p. 6054, 2020.

[15] A. K. Ghosh, D. L. Lubkeman, M. J. Downey, and R. H. Jones, "Distribution circuit state estimation using a probabilistic approach," *IEEE Transactions on Power Systems*, vol. 12, no. 1, pp. 45–51, 1997.

[16] M. E. Baran and A. W. Kelley, "State estimation for real-time monitoring of distribution systems," *IEEE Transactions on Power Systems*, vol. 9, no. 3, pp. 1601–1609, 1994.

[17] C. Lu, J. Teng, and W.-H. Liu, "Distribution system state estimation," *IEEE Transactions on Power systems*, vol. 10, no. 1, pp. 229–240, 1995.

[18] I. Roytelman and S. Shahidehpour, "State estimation for electric power distribution

systems in quasi real-time conditions," *IEEE Transactions on Power Delivery*, vol. 8, no. 4, pp. 2009–2015, 1993.

[19] M. E. Baran and A. W. Kelley, "A branch-current-based state estimation method for distribution systems," *IEEE transactions on power systems*, vol. 10, no. 1, pp. 483–491, 1995.

[20] K. A. Clements, "The impact of pseudo-measurements on state estimator accuracy," in *2011 IEEE Power and Energy Society General Meeting*. IEEE, 2011, pp. 1–4.

[21] E. Manitsas, R. Singh, B. C. Pal, and G. Strbac, "Distribution system state estimation using an artificial neural network approach for pseudo measurement modeling," *IEEE Transactions on Power Systems*, vol. 27, no. 4, pp. 1888–1896, 2012.

[22] M. Farrokhabadi and L. Vanfretti, "An efficient automated topology processor for state estimation of power transmission networks," *Electric power systems research*, vol. 106, pp. 188–202, 2014.

[23] E. Manitsas, R. Singh, B. Pal, and G. Strbac, "Modelling of pseudo-measurements for distribution system state estimation," 2008.

[24] M. Baran and T. McDermott, "Distribution system state estimation using ami data," in *2009 IEEE/PES Power Systems Conference and Exposition*. IEEE, 2009, pp. 1–3.

[25] R. F. Arritt, R. C. Dugan, R. W. Uluski, and T. F. Weaver, "Investigation load estimation methods with the use of ami metering for distribution system analysis," in *2012 Rural Electric Power Conference*. IEEE, 2012, pp. B3–1.

[26] G. López, J. Moreno, H. Amarís, and F. Salazar, "Paving the road toward smart grids through large-scale advanced metering infrastructures," *Electric Power Systems Research*, vol. 120, pp. 194–205, 2015.

[27] A. S. Meliopoulos, G. Cokkinides, and R. Webb, "Multiphase power flow analysis," in *Proceedings of Southeastcon*, 1982, pp. 270–275.

[28] A. S. Meliopoulos and F. Zhang, "Multiphase power flow and state estimation for

power distribution systems," *IEEE Transactions on Power Systems*, vol. 11, no. 2, pp. 939–946, 1996.

[29] R. Stevens, D. Rizy, and S. Purucker, "Performance of conventional power flow routines for real-time distribution automation applications," Oak Ridge National Lab., TN (USA), Tech. Rep., 1986.

[30] W.-M. Lin and J.-H. Teng, "Distribution fast decoupled state estimation by measurement pairing," *IEE Proceedings-Generation, Transmission and Distribution*, vol. 143, no. 1, pp. 43–48, 1996.

[31] B. Gou and A. Abur, "A direct numerical method for observability analysis," *IEEE Transactions on Power Systems*, vol. 15, no. 2, pp. 625–630, 2000.

[32] F. H. Magnago and A. Abur, "A unified approach to robust meter placement against loss of measurements and branch outages," in *Proceedings of the 21st International Conference on Power Industry Computer Applications. Connecting Utilities. PICA 99. To the Millennium and Beyond (Cat. No. 99CH36351)*. IEEE, 1999, pp. 3–8.

[33] B. Gou and A. Abur, "An improved measurement placement algorithm for network observability," *IEEE Transactions on Power Systems*, vol. 16, no. 4, pp. 819–824, 2001.

[34] R. Emami and A. Abur, "Robust measurement design by placing synchronized phasor measurements on network branches," *IEEE Transactions on power systems*, vol. 25, no. 1, pp. 38–43, 2009.

[35] X. Bei, Y. J. Yoon, and A. Abur, "Optimal placement and utilization of phasor measurements for state estimation," *PSERC Publication*, vol. 1, 2005.

[36] B. Xu and A. Abur, "Observability analysis and measurement placement for systems with pmus," in *IEEE PES Power Systems Conference and Exposition, 2004.* IEEE, 2004, pp. 943–946.

[37] K. Li, "State estimation for power distribution system and measurement impacts," *IEEE Transactions on Power Systems*, vol. 11, no. 2, pp. 911–916, 1996.

[38] J. Liu, J. Tang, F. Ponci, A. Monti, C. Muscas, and P. A. Pegoraro, "Trade-offs in pmu deployment for state estimation in active distribution grids," *IEEE transactions on Smart Grid*, vol. 3, no. 2, pp. 915–924, 2012.

[39] R. Singh, B. C. Pal, R. A. Jabr, and R. B. Vinter, "Meter placement for distribution system state estimation: An ordinal optimization approach," *IEEE Transactions on Power Systems*, vol. 26, no. 4, pp. 2328–2335, 2011.

[40] A. Gomez-Exposito, C. Gomez-Quiles, and I. Dzafic, "State estimation in two time scales for smart distribution systems," *IEEE Transactions on Smart Grid*, vol. 6, no. 1, pp. 421–430, 2014.

[41] A. Alimardani, F. Therrien, D. Atanackovic, J. Jatskevich, and E. Vaahedi, "Distribution system state estimation based on nonsynchronized smart meters," *IEEE Transactions on Smart Grid*, vol. 6, no. 6, pp. 2919–2928, 2015.

[42] X. Han, S. You, F. Thordarson, D. V. Tackie, S. M. Østberg, O. M. Pedersen, H. W. Bindner, and N. C. Nordentoft, "Real-time measurements and their effects on state estimation of distribution power system," in *IEEE PES ISGT Europe 2013*. IEEE, 2013, pp. 1–5.

[43] A. M. Stanković, V. Švenda, A. T. Sarić, and M. K. Transtrum, "Hybrid power system state estimation with irregular sampling," in *2017 IEEE Power & Energy Society General Meeting*. IEEE, 2017, pp. 1–5.

[44] P. Janssen, T. Sezi, and J.-C. Maun, "Distribution system state estimation using unsynchronized phasor measurements," in *2012 3rd IEEE PES Innovative Smart Grid Technologies Europe (ISGT Europe)*. IEEE, 2012, pp. 1–6.

[45] R. Singh, B. C. Pal, and R. A. Jabr, "Statistical representation of distribution system loads using gaussian mixture model," *IEEE Transactions on Power Systems*, vol. 25, no. 1, pp. 29–37, 2009.

[46] R. Singh, B. Pal, and R. Jabr, "Distribution system state estimation through gaussian mixture model of the load as pseudo-measurement," *IET generation, transmission & distribution*, vol. 4, no. 1, pp. 50–59, 2010.

[47] S. Nanchian, "State estimation for active distribution network," 2015.

[48] F. F. Wu and A. Monticelli, "Network observability: theory," *IEEE Transactions on Power Apparatus and Systems*, no. 5, pp. 1042–1048, 1985.

[49] Y. Wang, Q. Chen, T. Hong, and C. Kang, "Review of smart meter data analytics: Applications, methodologies, and challenges," *IEEE Transactions on Smart Grid*, vol. 10, no. 3, pp. 3125–3148, 2018.

[50] K. Gajowniczek and T. Zabkowski, "Short term electricity forecasting using individual smart meter data," *Procedia Computer Science*, vol. 35, pp. 589–597, 2014.

[51] T. C. Xygkis, G. D. Karlis, I. K. Siderakis, and G. N. Korres, "Use of near real-time and delayed smart meter data for distribution system load and state estimation," 2014.

[52] A. Al-Wakeel, J. Wu, and N. Jenkins, "State estimation of medium voltage distribution networks using smart meter measurements," *Applied energy*, vol. 184, pp. 207–218, 2016.

[53] R. Singh, "State estimation in power distribution network operation," 2009.

[54] X. Chen, K. J. Tseng, and G. Amaratunga, "State estimation for distribution systems using micro-synchrophasors," in *2015 IEEE PES Asia-Pacific Power and Energy Engineering Conference (APPEEC)*. IEEE, 2015, pp. 1–5.

[55] M. Gholami, A. Abbaspour, S. Fattaheian-Dehkordi, M. Lehtonen, M. Moeini-Aghtaie, and M. Fotuhi, "Optimal allocation of pmus in active distribution network considering reliability of state estimation results," *IET Generation, Transmission & Distribution*, vol. 14, no. 18, pp. 3641–3651, 2020.

[56] V. R. Disfani, M. C. Bozchalui, and R. Sharma, "Sdp-based state estimation of multi-phase active distribution networks using micro-pmus," *arXiv preprint arXiv:1504.03547*, 2015.

[57] M. T. Hagh, S. M. Mahaei, and K. Zare, "Improving bad data detection in state estimation of power systems," *International Journal of Electrical and Computer*

Engineering, vol. 1, no. 2, p. 85, 2011.

[58] F. F. Wu and W.-H. Liu, "Detection of topology errors by state estimation (power systems)," *IEEE Transactions on Power Systems*, vol. 4, no. 1, pp. 176–183, 1989.

[59] T. Van Cutsem, M. Ribbens-Pavella, and L. Mili, "Bad data identification methods in power system state estimation-a comparative study," *IEEE transactions on power apparatus and systems*, no. 11, pp. 3037–3049, 1985.

[60] F. F. Wu, W.-H. Liu, L. Holten, L. Gjelsvik, and S. Aam, "Observability analysis and bad data processing for state estimation using hachtel's augmented matrix method," *IEEE Transactions on Power Systems*, vol. 3, no. 2, pp. 604–611, 1988.

[61] J. Chen and A. Abur, "Placement of pmus to enable bad data detection in state estimation," *IEEE Transactions on Power Systems*, vol. 21, no. 4, pp. 1608–1615, 2006.

[62] A. Mutanen, A. Koto, A. Kulmala, and P. Jarventausta, "Development and testing of a branch current based distribution system state estimator," in *2011 46th International Universities' Power Engineering Conference (UPEC)*. VDE, 2011, pp. 1–6.

[63] D. Atanackovic and V. Dabic, "Deployment of real-time state estimator and load flow in bc hydro dms-challenges and opportunities," in *2013 IEEE Power & Energy Society General Meeting*. IEEE, 2013, pp. 1–5.

[64] R. Gonzalez, M. Bocos, J. Maza, E. Romero, I. Diaz, and A. Gastalver, "State estimation in mv distribution networks; experiences in the spanish smart grid project price," *Paris, CIGRE*, 2016.

[65] M. Pignati, M. Popovic, S. Barreto, R. Cherkaoui, G. D. Flores, J.-Y. Le Boudec, M. Mohiuddin, M. Paolone, P. Romano, S. Sarri *et al.*, "Real-time state estimation of the epfl-campus medium-voltage grid by using pmus," in *2015 IEEE Power & Energy Society Innovative Smart Grid Technologies Conference (ISGT)*. IEEE, 2015, pp. 1–5.

[66] L. Zanni, "Power-system state estimation based on pmus," 2017.

[67] S. Wang, X. Cui, Z. Li, and M. Shahidehpour, "An improved branch current-based

three-phase state estimation algorithm for distribution systems with dgs," in *IEEE PES Innovative Smart Grid Technologies*. IEEE, 2012, pp. 1–6.

[68] M. Pau, P. A. Pegoraro, and S. Sulis, "Efficient branch-current-based distribution system state estimation including synchronized measurements," *IEEE Transactions on Instrumentation and Measurement*, vol. 62, no. 9, pp. 2419–2429, 2013.

[69] R. Singh, B. Pal, and R. Jabr, "Choice of estimator for distribution system state estimation," *IET generation, transmission & distribution*, vol. 3, no. 7, pp. 666–678, 2009.

[70] F. C. Schweppe and E. J. Handschin, "Static state estimation in electric power systems," *Proceedings of the IEEE*, vol. 62, no. 7, pp. 972–982, 1974.

[71] M. Baran, "Branch current based state estimation for distribution system monitoring," in *2012 IEEE Power and Energy Society General Meeting*. IEEE, 2012, pp. 1–4.

[72] H. Wang and N. N. Schulz, "A revised branch current-based distribution system state estimation algorithm and meter placement impact," *IEEE Transactions on Power Systems*, vol. 19, no. 1, pp. 207–213, 2004.

[73] M. Pau, P. A. Pegoraro, and S. Sulis, "Wls distribution system state estimator based on voltages or branch-currents: Accuracy and performance comparison," in *2013 IEEE International Instrumentation and Measurement Technology Conference (I2MTC)*. IEEE, 2013, pp. 493–498.

[74] M. E. Baran, J. Jung, and T. E. McDermott, "Including voltage measurements in branch current state estimation for distribution systems," in *2009 IEEE Power & Energy Society General Meeting*. IEEE, 2009, pp. 1–5.

[75] W. Price, S. Casper, C. Nwankpa, R. Bradish, H. Chiang, C. Concordia, J. Staron, C. Taylor, E. Vaahedi, and G. Wu, "Bibliography on load models for power flow and dynamic performance simulation," *IEEE Power Engineering Review*, vol. 15, no. 2, p. 70, 1995.

[76] W. Price, C. Taylor, and G. Rogers, "Standard load models for power flow and dynamic

performance simulation," *IEEE Transactions on power systems*, vol. 10, no. CONF-940702-, 1995.

[77] D. P. Stojanović, L. M. Korunović, and J. Milanović, "Dynamic load modelling based on measurements in medium voltage distribution network," *Electric Power Systems Research*, vol. 78, no. 2, pp. 228–238, 2008.

[78] A. Arif, Z. Wang, J. Wang, B. Mather, H. Bashualdo, and D. Zhao, "Load modeling—a review," *IEEE Transactions on Smart Grid*, vol. 9, no. 6, pp. 5986–5999, 2017.

[79] F. F. Wu, "Power system state estimation: a survey," *International Journal of Electrical Power & Energy Systems*, vol. 12, no. 2, pp. 80–87, 1990.

[80] T. Van Cutsem and M. Ribbens-Pavella, "Critical survey of hierarchical methods for state estimation of electric power systems," *IEEE Transactions on Power Apparatus and Systems*, no. 10, pp. 3415–3424, 1983.

[81] A. Gómez-Expósito, A. de la Villa Jaén, C. Gómez-Quiles, P. Rousseaux, and T. Van Cutsem, "A taxonomy of multi-area state estimation methods," *Electric Power Systems Research*, vol. 81, no. 4, pp. 1060–1069, 2011.

[82] A. Da Silva, D. Falcao *et al.*, "Bibliography on power system state estimation (1968-1989)," *IEEE Transactions on Power Systems*, vol. 5, no. 3, pp. 950–961, 1990.

[83] J. Zhao, A. Gomez-Exposito, M. Netto, L. Mili, A. Abur, V. Terzija, I. Kamwa, B. C. Pal, A. K. Singh, J. Qi *et al.*, "Power system dynamic state estimation: motivations, definitions, methodologies and future work," *IEEE Transactions on Power Systems*, 2019.

[84] H. M. Beides and G. T. Heydt, "Dynamic state estimation of power system harmonics using kalman filter methodology," *IEEE Transactions on Power Delivery*, vol. 6, no. 4, pp. 1663–1670, 1991.

[85] R. E. Kalman *et al.*, "A new approach to linear filtering and prediction problems," *Journal of basic Engineering*, vol. 82, no. 1, pp. 35–45, 1960.

[86] C. Carquex, C. Rosenberg, and K. Bhattacharya, "State estimation in power distribution systems based on ensemble kalman filtering," *IEEE Transactions on Power Systems*, vol. 33, no. 6, pp. 6600–6610, 2018.

[87] B. Hayes and M. Prodanovic, "A comparison of mv distribution system state estimation methods using field data," in *2015 IEEE Power & Energy Society General Meeting*. IEEE, 2015, pp. 1–5.

[88] R. C. Francy, A. M. Farid, and K. Youcef-Toumi, "Event triggered state estimation techniques for power systems with integrated variable energy resources," *ISA transactions*, vol. 56, pp. 165–172, 2015.

[89] M. B. Do Coutto Filho and J. C. S. de Souza, "Forecasting-aided state estimation—part i: Panorama," *IEEE Transactions on Power Systems*, vol. 24, no. 4, pp. 1667–1677, 2009.

[90] M. B. Do Coutto Filho, J. C. S. de Souza, and R. S. Freund, "Forecasting-aided state estimation—part ii: Implementation," *IEEE Transactions on Power Systems*, vol. 24, no. 4, pp. 1678–1685, 2009.

[91] A. S. Debs and R. E. Larson, "A dynamic estimator for tracking the state of a power system," *IEEE Transactions on Power Apparatus and Systems*, no. 7, pp. 1670–1678, 1970.

[92] K. Nishiya, J. Hasegawa, and T. Koike, "Dynamic state estimation including anomaly detection and identification for power systems." *IEE Proceedings C. Generation, Transmission and Distribution*, vol. 129, pp. 192–198, 1982. [Online]. Available: http://search.proquest.com/docview/23386286/

[93] N. Zhou, D. Meng, Z. Huang, and G. Welch, "Dynamic state estimation of a synchronous machine using pmu data: A comparative study," *IEEE Transactions on Smart Grid*, vol. 6, no. 1, pp. 450–460, 2014.

[94] S. Sarri, M. Paolone, R. Cherkaoui, A. Borghetti, F. Napolitano, and C. A. Nucci, "State estimation of active distribution networks: Comparison between wls and iterated kalman-filter algorithm integrating pmus," in *2012 3rd IEEE PES Innovative Smart*

Grid Technologies Europe (ISGT Europe). IEEE, 2012, pp. 1–8.

[95] A. Bahgat, M. Sakr, and A. El-Shafei, "Two level dynamic state estimator for electric power systems based on nonlinear transformation," in *IEE Proceedings C (Generation, Transmission and Distribution)*, vol. 136, no. 1. IET, 1989, pp. 15–23.

[96] G. Valverde and V. Terzija, "Unscented kalman filter for power system dynamic state estimation," *IET generation, transmission & distribution*, vol. 5, no. 1, pp. 29–37, 2011.

[97] R. Gelagaev, P. Vermeyen, and J. Driesen, "State estimation in distribution grids," in *2008 13th International Conference on Harmonics and Quality of Power*. IEEE, 2008, pp. 1–6.

[98] Y. Zhang, J. Wang, and Z. Li, "Uncertainty modeling of distributed energy resources: techniques and challenges," *Current Sustainable/Renewable Energy Reports*, vol. 6, no. 2, pp. 42–51, 2019.

[99] W. L. Theo, J. S. Lim, W. S. Ho, H. Hashim, and C. T. Lee, "Review of distributed generation (dg) system planning and optimisation techniques: Comparison of numerical and mathematical modelling methods," *Renewable and Sustainable Energy Reviews*, vol. 67, pp. 531–573, 2017.

[100] C. Wang and M. H. Nehrir, "Analytical approaches for optimal placement of distributed generation sources in power systems," *IEEE Transactions on Power systems*, vol. 19, no. 4, pp. 2068–2076, 2004.

[101] P. S. Georgilakis and N. D. Hatziargyriou, "Optimal distributed generation placement in power distribution networks: models, methods, and future research," *IEEE Transactions on power systems*, vol. 28, no. 3, pp. 3420–3428, 2013.

[102] R. Al Abri, E. F. El-Saadany, and Y. M. Atwa, "Optimal placement and sizing method to improve the voltage stability margin in a distribution system using distributed generation," *IEEE transactions on power systems*, vol. 28, no. 1, pp. 326–334, 2012.

[103] J. Kennedy, "Particle swarm optimization," *Encyclopedia of machine learning*, pp. 760–766, 2010.

[104] M. E. Baran and F. F. Wu, "Network reconfiguration in distribution systems for loss reduction and load balancing," *IEEE Transactions on Power delivery*, vol. 4, no. 2, pp. 1401–1407, 1989.

[105] R. D. Zimmerman, C. E. Murillo-Sánchez, and D. Gan, "Matpower: A matlab power system simulation package," *Manual, Power Systems Engineering Research Center, Ithaca NY*, vol. 1, 1997.

[106] M. P. Lalitha, V. V. Reddy, and V. Usha, "Optimal dg placement for minimum real power loss in radial distribution systems using pso." *Journal of Theoretical & Applied Information Technology*, vol. 13, 2010.

[107] M. Chakravorty and D. Das, "Voltage stability analysis of radial distribution networks," *International Journal of Electrical Power & Energy Systems*, vol. 23, no. 2, pp. 129–135, 2001.

[108] A. Einfalt, A. Schuster, C. Leitinger, D. Tiefgraber, M. Litzlbauer, S. Ghaemi, D. Wertz, A. Frohner, and C. Karner, "Adres-concept: Konzeptentwicklung für adres-autonome dezentrale regenerative energiesysteme," *TU Wien, Institut für Elektrische Anlagen und Energiewirtschaft*, 2011.

[109] N. H. Abd Rahman and A. F. Zobaa, "Integrated mutation strategy with modified binary pso algorithm for optimal pmus placement," *IEEE Transactions on Industrial Informatics*, vol. 13, no. 6, pp. 3124–3133, 2017.

[110] M. Ahmad, *Power system state estimation.* Artech House, 2013.

[111] E. Caro, R. Mínguez, and A. J. Conejo, "Robust wls estimator using reweighting techniques for electric energy systems," *Electric Power Systems Research*, vol. 104, pp. 9–17, 2013.

[112] D. P. Kothari and I. Nagrath, *Modern power system analysis.* Tata McGraw-Hill Education, 1989.

[113] M. Paolone, J. Y. Le Boudec, S. Sarri, and L. Zanni, "Static and recursive pmu based state estimation processes for transmission and distribution power grids," The

Institution of Engineering and Technology-IET, Tech. Rep., 2015.

Appendix A

IEEE 33-bus test system data

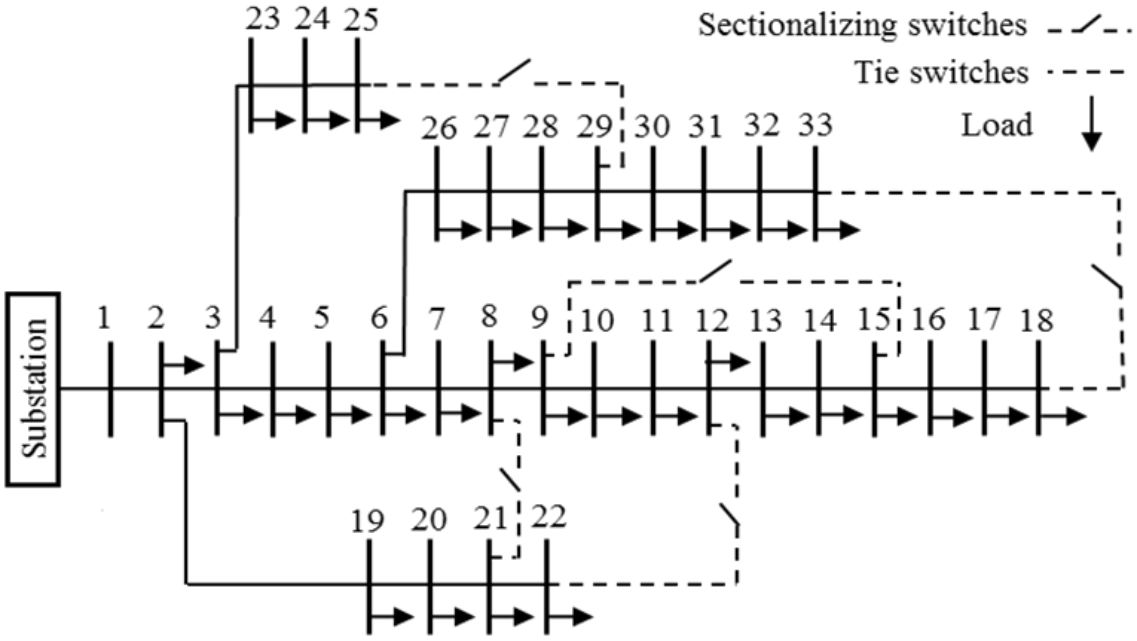

IEEE 33-bus test system single-line diagram

Table A.1: System data for IEEE 33-bus test system

S_base (MVA)	V_base (kV)	Z_base (ohms)	Resistance and Reactance (ohms)		Resistance and Reactance (pu)*		Conductance and Susceptance (pu)*		Maximum Line Capacity	
100	**12.66**	**1.602756**								
	From	**To**	**R (ohms)**	**X (ohms)**	**R (pu)**	**X (pu)**	**G (pu)**	**B (pu)**	**P (KW)**	**Q (KVAR)**
	1	2	0.0922	0.0470	0.0575	0.0293	13.7980	-7.0337	4600	4600
	2	3	0.4930	0.2511	0.3076	0.1567	2.5814	-1.3148	4100	4100
	3	4	0.3660	0.1864	0.2284	0.1163	3.4772	-1.7709	2900	2900
	4	5	0.3811	0.1941	0.2378	0.1211	3.3394	-1.7008	2900	2900
	5	6	0.8190	0.7070	0.5110	0.4411	1.1213	-0.9680	2900	2900
	6	7	0.1872	0.6188	0.1168	0.3861	0.7179	-2.3729	1500	1500
	7	8	0.7114	0.2351	0.4439	0.1467	2.0311	-0.6712	1050	1050
	8	9	1.0300	0.7400	0.6426	0.4617	1.0263	-0.7374	1050	1050
	9	10	1.0440	0.7400	0.6514	0.4617	1.0218	-0.7243	1050	1050
	10	11	0.1966	0.0650	0.1227	0.0406	7.3490	-2.4297	1050	1050
	11	12	0.3744	0.1298	0.2336	0.0810	3.8215	-1.3249	1050	1050
	12	13	1.4680	1.1550	0.9159	0.7206	0.6744	-0.5306	500	500
	13	14	0.5416	0.7129	0.3379	0.4448	1.0830	-1.4255	450	450
	14	15	0.5910	0.5260	0.3687	0.3282	1.5132	-1.3468	300	300
	15	16	0.7463	0.5450	0.4656	0.3400	1.4006	-1.0228	250	250
	16	17	1.2890	1.7210	0.8042	1.0738	0.4469	-0.5966	250	250
	17	18	0.7320	0.5740	0.4567	0.3581	1.3559	-1.0632	100	100
	2	19	0.1640	0.1565	0.1023	0.0976	5.1150	-4.8811	500	500
	19	20	1.5042	1.3554	0.9385	0.8457	0.5881	-0.5299	500	500
	20	21	0.4095	0.4784	0.2555	0.2985	1.6551	-1.9335	210	210
	21	22	0.7089	0.9373	0.4423	0.5848	0.8227	-1.0878	110	110
	3	23	0.4512	0.3083	0.2815	0.1924	2.4216	-1.6547	1050	1050
	23	24	0.8980	0.7091	0.5603	0.4424	1.0993	-0.8681	1050	1050
	24	25	0.8960	0.7011	0.5590	0.4374	1.1095	-0.8681	500	500
	6	26	0.2030	0.1034	0.1267	0.0645	6.2689	-3.1931	1500	1500
	26	27	0.2842	0.1447	0.1773	0.0903	4.4786	-2.2802	1500	1500
	27	28	1.0590	0.9337	0.6607	0.5826	0.8515	-0.7508	1500	1500
	28	29	0.8042	0.7006	0.5018	0.4371	1.1331	-0.9871	1500	1500
	29	30	0.5075	0.2585	0.3166	0.1613	2.5076	-1.2772	1500	1500
	30	31	0.9744	0.9630	0.6080	0.6008	0.8321	-0.8224	500	500
	31	32	0.3105	0.3619	0.1937	0.2258	2.1886	-2.5509	500	500
	32	33	0.3410	0.5302	0.2128	0.3308	1.3753	-2.1384	100	100

Table A.2: IEEE 33-bus test system load data

Bus Number	**Nominal load**	
	P (KW)	**Q(KVAR)**
1	0	0
2	100	60
3	90	40
4	120	80
5	60	30
6	60	20
7	200	100
8	200	100
9	60	20
10	60	20
11	45	30
12	60	35
13	60	35
14	120	80
15	60	10
16	60	20
17	60	20
18	90	40
19	90	40
20	90	40
21	90	40
22	90	40
23	90	50
24	420	200
25	420	200
26	60	25
27	60	25
28	60	20
29	120	70
30	200	600
31	150	70
32	210	100
33	60	40

Appendix B

MATLAB Code

```
%running the IEEE-33 bus system SE in MATLAB & OpenDSS
clear
clc



%% setting up OpenDSS
text = pwd;%current path
dss_path = [text, '\master33Full.dss'];
disp(dss_path);

[DSSObj, flag] = DSSStartup(dss_path);
% the OpenDSS Object allows interacting with the COM interface
% flag is set when the object is successfully instantiated
if ¬flag
    error('Fatal error!\n Failed to create the COM object to interface ...
        with OpenDSS');
end

% DSSText=DSSObj.text;
% DSSCircuit=DSSObj.ActiveCircuit;
% DSSText.Command='Set mode=snapshot';
% DSSText.Command='solve';
% DSSText.command='show voltages';

```

```
%% Getting Ybus matrix
%manual Ybus
Y=manualYMatrix33ph;

%% Defining loads over simulation period
%base case loads
Pref=[100;90;120;60;60;200;200;60;60;45;60;60;120;60;60;60;90;90;90;90;90;90; ...
    420;420;60;60;60;120;200;150;210;60];
Qref=[60;40;80;30;20;100;100;20;20;30;35;35;80;10;20;20;40;40;40;40;40;50;
200;200;25;25;20;70;600;70;100;40];

secNodes=55;%number of load nodes in the secondary power system
dur=3600;% the pseudo meas. will be available for every dur seconds
%Assigne load curves to nodes (using ADRES data set)
%getting the required load indices for connecting houses to secondary nodes
%and getting predicted loads for the next day
factor=10;
% [P,Q,delayedP,delayedQ,PpMean,PpStd,QpMean,QpStd,PdiffStd,QdiffStd,Ppsi,
Qpsi]=loadProcessAssignHalf1ph1(Pref,secNodes,dur,resol,delay,factor);
% [P,Q]=loadProcessAssign1ph1Week(Pref,secNodes,dur,resol,delay,factor);
caseName = ['newLoadF10D1R' num2str(resol) 'Dur3600'];
load(caseName)
if delay == 0
    delayedP = P;
    delayedQ = Q;
end
% PpMean=PpMean/3;
% PpStd=PpStd/3;
% PdiffStd=PdiffStd/3;
% QpMean=QpMean/3;
% QpStd=QpStd/3;
% QdiffStd=QdiffStd/3;

%% perunit values
sBase=100e3/3; %single phase power base
vBasePri=12.66e3/sqrt(3); %single phase primary network voltage base
vBaseSec=.416/sqrt(3); %single phase secondary network voltage base
yBase=sBase/vBasePri^2;
priNodes=33*3; %all 3 phases
Y=Y/yBase;
Ibase=sBase/vBasePri;
% secNodes=32*110;

```

```
%% initialization
%assume the following nodes have PMUs
PMUmap=[1,33,32,31,18,17,30,16,29,15,14,13,28,12,11,10,9,8,27,26,7,6,25,24,
5,4,23,3,22,21,20,19,2];
PMUnodes=sort(PMUmap(1:PMUnumber+1));
% PMUnodes=[1,33,18,22,25,12,6,3,29,9,15];
% PMUnodes=[1,33,18,22,25,6];
% PMUnodes=[1,33,18,22,25,6,3,31,29,27,20,26,14,12,10,8,4,24,23,4,2];
% PMUnodes=[1,33,18];
iter=zeros(1,length(P(1,:)));
V_WLS=zeros(length(P(1,:)),priNodes);
MSE_WLS=zeros(1,length(P(1,:)));
%EKF
L=500;%ensemble size
X=zeros(2*length(PpMean(:,1)),L);
hX=zeros(2*3*length(PMUnodes),L);
Xave=zeros(2*length(PpMean(:,1)),length(P(1,:)));
V_EKF=zeros(length(P(1,:)),priNodes);
MSE_EKF=zeros(1,length(P(1,:)));
%PMUs at all nodes
MSE_PMU=zeros(1,length(P(1,:)));

%loading loadflow results
% load('LoadFlowResultsR60.mat');

%% main loop
for k=1:length(P(1,:))
    disp("hour: "+ k);
%     %% setting up OpenDSS
    text = pwd;%current path
    dss_path = [text, '\master33Full.dss'];
    [DSSObj, flag] = DSSStartup(dss_path);
    % the OpenDSS Object alows interacting with the COM interface
    % flag is set when the object is successfully instantiated
    if ¬flag
        error('Fatal error!\n Failed to create the COM object to ...
           interface with OpenDSS');
    end
    %% Running the power flow
    [Vtrue, lineCurrent, ¬, ¬]=runPFfull(DSSObj,P(:,k),Q(:,k));
    [Vdelayed, lineCurrentDelayed, ¬, ¬...
       ]=runPFfull(DSSObj,delayedP(:,k),delayedQ(:,k));

```

```
108     % calculating load power at each primary bus
109     % method 1: adding the load powers together
110     PseudoLoadPower=zeros(32*3,3);
111     PseudoLoadPower(:,1)=4:33*3;
112     PseudoLoadPower(:,2)=PpMean(:,ceil(k*resol/dur));%pseudo measurment ...
            Ppseudo
113     PseudoLoadPower(:,3)=QpMean(:,ceil(k*resol/dur));%pseudo measurment ...
            Qpseudo
114
115     %% converting to per-unit
116     Vtrue(1:priNodes)=Vtrue(1:priNodes)/vBasePri;
117     Vtrue(priNodes+1:end)=Vtrue(priNodes+1:end)/vBaseSec*sqrt(3);
118 %     linePowerTransfer(:,[3,4])=linePowerTransfer(:,[3,4])/sBase;
119     PseudoLoadPower(:,[2,3])=PseudoLoadPower(:,[2,3])/sBase*1000;
120     %PseudoLoadPower is in kW
121     VtruePrim=Vtrue(1:priNodes);%getting the primary nodes voltages
122     disp("initial error: "+ ...
            sqrt(1/99*sum(abs(VtruePrim-repmat([1,exp(-2*pi*1i/3),exp(-4*pi*1i/3)]
123
124     VdelayedPrim=Vdelayed(1:priNodes)/vBasePri;
125
126
127     %% adding noise
128     rdnV=sigmaPMU*randn(1,length(VtruePrim));%adding noise to magnitude ...
            only
129     for rr=1:length(rdnV)
130         alpha=rand*2*pi;
131         rdnV(rr)=rdnV(rr)*(cos(alpha)+1i*sin(alpha));
132     end
133     % calculate the max angle difference
134     Vnoisy=VdelayedPrim+rdnV;%adding total vector error
135     VnoisyAngleDiff=max(angle(Vnoisy)-angle(VdelayedPrim));
136     if currentPhasor == true
137         %per unit
138         lineCurrentDelayed(:,3:8)=lineCurrentDelayed(:,3:8)/Ibase;
139         %adding noise to current readings
140         rdnI=sigmaPMU/sqrt(2)*randn(2*32,6);
141         lineCurrentNoisy=lineCurrentDelayed(:,1:2);
142         lineCurrentNoisy(:,3:8)=0;
143         lineCurrentNoisy(:,3:8)=lineCurrentDelayed(:,3:8).*(1+rdnI);
144     else
145         lineCurrentNoisy = [];
146     end
```

```
147 %     %load flow results
148 %     Vnoisy=AllVnoisy(k,:);
149 %     lineCurrentNoisy=AllLineCurrentNoisy(:,:,k);
150 %     if delay==1
151 %         VtruePrim=AllVtruePrim(k,:);
152 %     else
153 %         VtruePrim=AllVdelayedPrim(k,:);
154 %     end
155
156     %covariance matrix of the error
157     if currentPhasor == true
158         R=diag([PpStd(:,ceil(k*resol/dur)).'.^2,QpStd(:,ceil(k*resol/dur))
159         .'.^2
160         ,...%Pseudo measurements
161             sigmaPMU^2*ones(1,3*2*length(PMUnodes)-1),...%PMU voltage ...
                    measurement
162             sigmaPMU^2*ones(1,3*2*length(PMUnodes))]);%PMU current ...
                    measurement
163     else
164         R=diag([PpStd(:,ceil(k*resol/dur)).'.^2,QpStd(:,ceil(k*resol/dur)).'.^2,
165         ...%Pseudo measurements
166             sigmaPMU^2*ones(1,3*2*length(PMUnodes)-1)]);
167     end
168
169     %error if we had PMUs at all nodes
170     MSE_PMU(k)=(1/99*sum(abs(VtruePrim-Vnoisy).^2));
171
172
173     %% Defining measurement data for WLS SE
174     % [z,zType]=getMeasurements(Vtrue, linePowerTransfer, ...
            PseudoLoadPower);%for testing the accuracy of WLS method without ...
            any noise
175     [z,zType]=getMeasurements(Vnoisy, lineCurrentNoisy, ...
            PseudoLoadPower, PMUnodes, currentPhasor);%WLS with noisy data
176
177     %% performing WLS SE
178     iter_max=10;
179     threshold=1e-7;%stopping criteria: WLS stopes when Δ_x is smaller ...
            than threshold or iteration number>iter_max
180     exit=0;
181     while exit<3
182         [V_WLS(k,:),iter(k)]=WLS_SE(Y,z,zType,R,iter_max,threshold,VtruePrim);
183         if iter(k)>1
```

```
184             exit=3;
185         else
186             exit=exit+1;
187         end
188     end
189     disp("iteration number: "+ iter(k));
190     %result error
191     MSE_WLS(k)=(1/99*sum(abs(VtruePrim-V_WLS(k,:)).^2));
192     disp("WLS: RMS error in voltage phasors: "+ sqrt(MSE_WLS(k)));
193
194     %% setting up OpenDSS for EKF
195     text = pwd;%current path
196     dss_path = [text, '\master33.dss'];
197     [DSSObj, flag] = DSSStartup(dss_path);
198     % the OpenDSS Object alows interacting with the COM interface
199     % flag is set when the object is successfully instantiated
200     if ¬flag
201         error('Fatal error!\n Failed to create the COM object to ...
                interface with OpenDSS');
202     end
203
204
205     %% EKF
206     if k==1
207         %initialization
208         X(:,:)=[PpMean(:,k);QpMean(:,k)]+[PpStd(:,k).*randn(length(PpMean
209         (:,1)),L);QpStd(:,k).*randn(length(PpMean(:,1)),L)];
210     else
211         %state integration
212         X(:,:)=X(:,:)+[PdiffStd(:,1).*randn(length(PdiffStd(:,1)),L);QdiffStd
213         (:,1).*randn(length(QdiffStd(:,1)),L)];
214     end
215     %% Pseudo measurement assimilation
216     pseudoStep=ceil(k*resol/dur);
217     PSI=diag([Ppsi(:,pseudoStep);Qpsi(:,pseudoStep)]);
218     QModel=diag([PdiffStd(:,1).^2;QdiffStd(:,1).^2]);
219     R=diag([PpStd(:,pseudoStep).^2;QpStd(:,pseudoStep).^2]);
220     H=eye(length(PSI));
221
222     d=[PpMean(:,pseudoStep);QpMean(:,pseudoStep)];%pseudo measurement
223     D=d+[PpStd(:,pseudoStep).*randn(32*3,L);QpStd(:,pseudoStep).*randn(32*3,L)];
224     %intermediary matrices
225     H∆=H-PSI*H;
```

```
226     C=QModel*H.'*PSI.';
227     DΔ=D-PSI*D;
228     RΔ=R-PSI*R*PSI.'+PSI*H*QModel*H.'*PSI.';
229     %update equations
230     Xp=X(:,:);
231     E_X=mean(Xp,2);
232     covXp=(Xp-E_X)*(Xp-E_X).';
233     E=HΔ*covXp*HΔ.'+RΔ+HΔ*C+C.'*HΔ.';
234     K=(covXp*HΔ.'+C)*E^-1;
235     Xu=Xp+K*(DΔ-HΔ*Xp);
236
237
238     % now we need to do a load flow
239     for l=1:L
240         %load flow
241         [Vxl,Ixl]=runPF(DSSObj,Xu(1:length(PpMean(:,1)),l),Xu(length(PpMean
242         (:,1))+1:end,l));
243         Vxl=Vxl/vBasePri;
244         hX(:,l)=[abs(Vxl(PMUnodes1ph))';angle(Vxl(PMUnodes1ph))'];
245     end
246     %Augmented  X_hat
247     X_hat=[Xu;hX];
248     %defining H_hat
249     H_hat=[zeros(2*length(PMUnodes1ph),2*length(PpMean(:,1))),diag(ones(1,
250     2*length(PMUnodes1ph)))];
251     %calculating Kalman Filter K
252     E_X=mean(Xu,2);
253     E_HX=mean(H_hat*X_hat,2);
254     E_Z=mean(Z,2);
255     K=(Xu-E_X)*(H_hat*X_hat-E_HX).'*...
256         ((H_hat*X_hat-E_HX)*(H_hat*X_hat-E_HX).'+(Z-E_Z)*(Z-E_Z).')^-1;
257     %Calculating Xa at iteration k
258     Xa=Xu+K*(Z-H_hat*X_hat);
259     %%%%%%%%%%%%%%%%%%%%%%%%%%%%%%%%%%%%%%%%%%%%%%%%%%%%%%%%%%%%%%%%%%%%%%%%
260     if currentPhasor == true
261         %PMU Current phasor assimilation
262         PMUCurrentMap=[1,2:2:64];
263         PMU_Iidx=PMUCurrentMap(PMUnodes);
264         ZI_PMU=[lineCurrentNoisy(PMU_Iidx,3:2:7);lineCurrentNoisy(PMU_Iidx,
265         4:2:8)];
266         ZI_PMU=reshape(ZI_PMU.',[],1);
267         Z=ZI_PMU.*(1+sigmaPMU/sqrt(2)*randn(length(ZI_PMU),L));
268         % now we need to do a load flow for each ensemble of Xa
```

```
269         for l=1:L
270             %load flow
271             [Vxl,Ixl]=runPF(DSSObj,Xa(1:length(PpMean(:,1)),l),Xa(length(PpMean
272             (:,1))+1:end,l));
273             Ixl(:,3:8)=Ixl(:,3:8)/Ibase;
274             Ixl_PMU=[Ixl(PMU_Iidx,3:2:7);Ixl(PMU_Iidx,4:2:8)];
275             hX(:,l)=reshape(Ixl_PMU.',[],1);
276         end
277     end
278     %Augmented X_hat
279     X_hat=[Xa;hX];
280     %defining H_hat
281     H_hat=[zeros(2*length(PMUnodes1ph),2*length(PpMean(:,1))),diag(ones(1,
282     2*length(PMUnodes1ph)))];
283     %calculating Kalman Filter K
284     E_X=mean(Xa,2);
285     E_HX=mean(H_hat*X_hat,2);
286     E_Z=mean(Z,2);
287     K=(Xa-E_X)*(H_hat*X_hat-E_HX).'*...
288         ((H_hat*X_hat-E_HX)*(H_hat*X_hat-E_HX).'+(Z-E_Z)*(Z-E_Z).')^-1;
289     %Calculating Xa at iteration k
290     Xa=Xa+K*(Z-H_hat*X_hat);
291
292     %% replacing X_k with Xa_k
293     X(:,:)=Xa;
294     %averaging
295     Xave(:,k)=mean(X(:,:),2);
296     %do a final load flow to get the node voltages
297     V_EKF(k,:)=runPF(DSSObj,Xave(1:length(PpMean
298     (:,1)),k),Xave(length(PpMean(:,1))+1:end,k));
299     V_EKF(k,:)=V_EKF(k,:)/vBasePri;
300     MSE_EKF(k)=(1/99*sum(abs(VtruePrim-V_EKF(k,:)).^2));
301     disp("EKF: RMS error in voltage phasors: "+ sqrt(MSE_EKF(k)));
302 end
303
304
305 disp("Average RMS Error WLS: "+ sqrt(mean(MSE_WLS)));
306 disp("Average RMS Error EKF: "+ sqrt(mean(MSE_EKF)));
```

Appendix C

IEEE-69 test bus system data

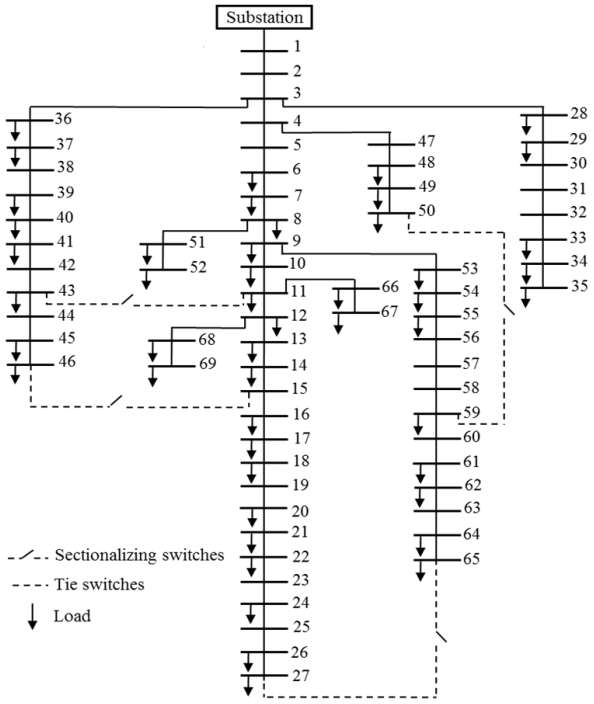

IEEE=69 Bus Single-Line Diagram

Table C.1: System data for 69-Bus radial distribution network

S_base (MVA)	V_base (kV)	Z_base (ohms)	Resistance and Reactance (ohms)		Resistance and Reactance (pu)*		Conductance and Susceptance (pu)*		Maximum Line Capacity
100	12.66	1.6028							
Branch Number	From	To	Resistance (ohms)	Reactance (ohms)	R (pu)	X (pu)	G (pu)	B (pu)	S (KVA)
	1	2	0.0005	0.0012	0.0003	0.0007	474.1882	-1138.0516	10761
	2	3	0.0005	0.0012	0.0003	0.0007	474.1882	-1138.0516	10761
	3	4	0.0015	0.0036	0.0009	0.0022	158.0627	-379.3505	10761
	4	5	0.0251	0.0294	0.0157	0.0183	26.9205	-31.5324	5823
	5	6	0.3660	0.1864	0.2284	0.1163	3.4772	-1.7709	1899
	6	7	0.3811	0.1941	0.2378	0.1211	3.3394	-1.7008	1899
	7	8	0.0922	0.0470	0.0575	0.0293	13.7980	-7.0337	1899
	8	9	0.0493	0.0251	0.0308	0.0157	25.8180	-13.1446	1899
	9	10	0.8190	0.2707	0.5110	0.1689	1.7642	-0.5831	1455
	10	11	0.1872	0.0619	0.1168	0.0386	7.7179	-2.5520	1455
	11	12	0.7114	0.2351	0.4439	0.1467	2.0311	-0.6712	1455
	12	13	1.0300	0.3400	0.6426	0.2121	1.4032	-0.4632	1455
	13	14	1.0440	0.3450	0.6514	0.2153	1.3841	-0.4574	1455
	14	15	1.0580	0.3496	0.6601	0.2181	1.3658	-0.4513	1455
	15	16	0.1966	0.0650	0.1227	0.0406	7.3490	-2.4297	1455
	16	17	0.3744	0.1238	0.2336	0.0772	3.8589	-1.2760	1455
	17	18	0.0047	0.0016	0.0029	0.0010	305.5965	-104.0328	2200
	18	19	0.3276	0.1083	0.2044	0.0676	4.4104	-1.4580	1455
	19	20	0.2106	0.0690	0.1314	0.0431	6.8727	-2.2517	1455
	20	21	0.3416	0.1129	0.2131	0.0704	4.2299	-1.3980	1455
	21	22	0.0140	0.0046	0.0087	0.0029	103.3274	-33.9504	1455
	22	23	0.1591	0.0526	0.0993	0.0328	9.0813	-3.0024	1455
	23	24	0.3463	0.1145	0.2161	0.0714	4.1721	-1.3795	1455
	24	25	0.7488	0.2475	0.4672	0.1544	1.9296	-0.6378	1455
	25	26	0.3089	0.1021	0.1927	0.0637	4.6776	-1.5461	1455
	26	27	0.1732	0.0572	0.1081	0.0357	8.3438	-2.7556	1455
	3	28	0.0044	0.0108	0.0027	0.0067	51.8539	-127.2777	10761
	28	29	0.0640	0.1565	0.0399	0.0976	3.5881	-8.7739	10761
	29	30	0.3978	0.1315	0.2482	0.0820	3.6321	-1.2007	1455
	30	31	0.0702	0.0232	0.0438	0.0145	20.5832	-6.8024	1455
	31	32	0.3510	0.1160	0.2190	0.0724	4.1166	-1.3605	1455
	32	33	0.8390	0.2816	0.5235	0.1757	1.7169	-0.5763	2200
	33	34	1.7080	0.5646	1.0657	0.3523	0.8459	-0.2796	1455
	34	35	1.4740	0.4873	0.9197	0.3040	0.9802	-0.3241	1455
	3	36	0.0044	0.0108	0.0027	0.0067	51.8539	-127.2777	10761
	36	37	0.0640	0.1565	0.0399	0.0976	3.5881	-8.7739	10761
	37	38	0.1053	0.1230	0.0657	0.0767	6.4374	-7.5195	5823
	38	39	0.0304	0.0355	0.0190	0.0221	22.3052	-26.0472	5823
	39	40	0.0018	0.0021	0.0011	0.0013	377.1191	-439.9722	5823
	40	41	0.7283	0.8509	0.4544	0.5309	0.9305	-1.0872	5823
	41	42	0.3100	0.3623	0.1934	0.2260	2.1853	-2.5540	5823
	42	43	0.0410	0.0478	0.0256	0.0298	16.5698	-19.3179	5823
	43	44	0.0092	0.0116	0.0057	0.0072	67.2690	-84.8174	5823
	44	45	0.1089	0.1373	0.0679	0.0857	5.6834	-7.1656	5823
	45	46	0.0009	0.0012	0.0006	0.0007	641.1024	-854.8032	6709
	4	47	0.0034	0.0084	0.0021	0.0052	66.3586	-163.9448	10761
	47	48	0.0851	0.2083	0.0531	0.1300	2.6939	-6.5939	10761
	48	49	0.2898	0.7091	0.1808	0.4424	0.7915	-1.9368	10761
	49	50	0.0822	0.2011	0.0513	0.1255	2.7914	-6.8290	10761
	8	51	0.0928	0.0473	0.0579	0.0295	13.7095	-6.9877	1899
	51	52	0.3319	0.1114	0.2071	0.0695	4.3401	-1.4567	2200
	52	53	0.1740	0.0886	0.1086	0.0553	7.3147	-3.7246	1899
	53	54	0.2030	0.1034	0.1267	0.0645	6.2689	-3.1931	1899
	54	55	0.2842	0.1447	0.1773	0.0903	4.4786	-2.2802	1899
	55	56	0.2813	0.1433	0.1755	0.0894	4.5237	-2.3045	1899
	56	57	1.5900	0.5337	0.9920	0.3330	0.9060	-0.3041	2200
	57	58	0.7837	0.2630	0.4890	0.1641	1.8381	-0.6168	2200
	58	59	0.3042	0.1006	0.1898	0.0628	4.7493	-1.5706	1455
	59	60	0.3861	0.1172	0.2409	0.0731	3.8009	-1.1538	1455
	60	61	0.5075	0.2585	0.3166	0.1613	2.5076	-1.2772	1899
	61	62	0.0974	0.0496	0.0608	0.0309	13.0668	-6.6542	1899
	62	63	0.1450	0.0738	0.0905	0.0460	8.7793	-4.4683	1899
	63	64	0.7105	0.3619	0.4433	0.2258	1.7911	-0.9123	1899
	64	65	1.0410	0.5302	0.6495	0.3308	1.2225	-0.6226	1899
	11	66	0.2012	0.0611	0.1255	0.0381	7.2934	-2.2148	1455
	66	67	0.0047	0.0014	0.0029	0.0009	313.2205	-93.2997	1455
	12	68	0.7394	0.2444	0.4613	0.1525	1.9541	-0.6459	1455
	68	69	0.0047	0.0016	0.0029	0.0010	305.5965	-104.0328	1455

Table C.2: IEEE-69 bus data set

Bus Number	Nominal load	
	P (KW)	Q(KVAR)
1	0	0
2	0	0
3	0	0
4	0	0
5	0	0
6	2.6	2.2
7	40.4	30
8	75	54
9	30	22
10	28	19
11	145	104
12	145	104
13	8	5
14	8	5.5
15	0	0
16	45.5	30
17	60	35
18	60	35
19	0	0
20	1	0.6
21	114	81
22	5	3.5
23	0	0
24	28	20
25	0	0
26	14	10
27	14	10
28	26	18.6
29	26	18.6
30	0	0
31	0	0
32	0	0
33	14	10
34	9.5	14
35	6	4
36	26	18.55
37	26	18.55
38	0	0
39	24	17
40	24	17
41	1.2	1
42	0	0
43	6	4.3
44	0	0
45	39.22	26.3
46	39.22	26.3
47	0	0
48	79	56.4
49	384.7	274.5
50	384.7	274.5
51	40.5	28.3
52	3.6	2.7
53	4.35	3.5
54	26.4	19
55	24	17.2
56	0	0
57	0	0
58	0	0
59	100	72
60	0	0
61	1244	888
62	32	23
63	0	0
64	227	162
65	59	42
66	18	13
67	18	13
68	28	20
69	28	20